1962

A Study of the Influences of Bayer Process Impurities on the Crystallization of Alumina Trihydrate.

James Leslie Kelly
Louisiana State University and Agricultural & Mechanical College

A STUDY OF THE INFLUENCES OF BAYER PROCESS IMPURITIES ON THE CRYSTALLIZATION OF ALUMINA TRIHYDRATE

A Dissertation

Submitted to the Graduate Faculty of the
Louisiana State University and
Agricultural and Mechanical College
in partial fulfillment of the
requirements for the degree of
Doctor of Philosophy

in

The Department of Chemical Engineering

by
James Leslie Kelly
B.S., Tulane University, 1954
M.S., Louisiana State University, 1960
June, 1962

ACKNOWLEDGMENT

Sincere appreciation is extended to those persons and organizations who provided their valuable assistance in the course of this research and in the preparation of this dissertation. To be particularly mentioned are Dr. Arthur G. Keller for his guidance; Messrs. L. M. Carpenter, L. M. Dunlap, and G. H. Sexton for their assistance with the apparatus; the National Council for Stream Improvement and the Coastal Studies Institute for the use of their laboratory facilities; Ormet Corporation for technical assistance; Union Carbide and Nuclear Company for microphotographic work and the typing of this dissertation; and Kaiser Aluminum and Chemical Corporation for technical assistance and the financial support of this study.

TABLE OF CONTENTS

LIST OF TABLES

LIST OF FIGURES

ABSTRACT

In the production of alumina by the Bayer process, one of the more important phases of the process is the precipitation step, wherein supersaturated sodium aluminate solutions decompose to ultimately yield alumina trihydrate crystals and sodium hydroxide. It is suspected that this precipitation reaction may be significantly influenced by various impurities present in Bayer plant liquors. (In this paper, all components present in Bayer liquors other than sodium hydroxide, sodium aluminate, aluminum hydroxide, alumina hydrate and water are referred to as impurities.) An understanding of the effects exerted by these impurities on the crystallization of alumina trihydrate is prerequisite to the most economical operation of Bayer plants. To acquire such an understanding, this research was initiated.

The effects of three impurities were investigated: sodium oxalate, soluble starch, and magnesium. All of these occur to varying degrees in typical Bayer plant liquors. Each impurity was studied individually in otherwise pure standard sodium aluminate solutions, containing initially 40 gpl NaOH and 16.2 gpl aluminum. Reagent grade NaOH and 99.99% Al were used to make up the standard solutions. Reagent grade $Na_2C_2O_4$, soluble starch, and $4MgCO_3 \cdot Mg(OH)_2 \cdot 5H_2O$ were used as impurities. The standard solutions were charged with seed and the impurity to be investigated, and were allowed to decompose isothermally ($70^{\circ}C$) under conditions of constant agitation. Electrical resistance-vs-time data were obtained during decomposition. Final aluminum concentrations and sieve analyses

of product crystals were determined. This data permitted determination of the impurity influences on induction periods, initial decomposition rates, "equilibrium concentrations," and crystal sizes. Microphotographs of the product crystals are presented.

For the concentrations studied, it was concluded that (1) sodium oxalate has unimportant effects on the crystallization step; (2) starch significantly affects the crystallization step, resulting in prolonged induction periods, decreased decomposition rates, higher "equilibrium concentrations," and coarser products; and (3) magnesium has little effect on either induction periods or product sizes but quite significantly decreases decomposition rates and increases "equilibrium concentrations." These results were interpreted to explain theoretically the mechanisms involved.

CHAPTER I

INTRODUCTION

Alumina, Al_2O_3, is obtained principally via the Bayer process from bauxite, an ore formed by the weathering of aluminum-bearing rocks. In essence, the Bayer process consists of digesting bauxite in a concentrated solution of caustic soda (NaOH) at elevated temperatures to yield a saturated solution of sodium aluminate and a large quantity of undissolved and undesired solids. After removal of most of these solids by sedimentation and filtration techniques the solution is flashed to a lower temperature, thereby becoming highly supersaturated. This supersaturated solution is pumped into large precipitation tanks. In these tanks, in the presence of previously precipitated alumina trihydrate seed which must be added, the sodium aluminate solution cools and decomposes to caustic soda and crystalline alumina trihydrate. The final step of the Bayer process is to separate the newly precipitated trihydrate from the liquor and subsequently to dehydrate it to alumina. The process may be conveniently represented by three equations:

$$Al_2O_3 \cdot 3H_2O + 2NaOH \xrightarrow{\text{Digestion}} 2NaAlO_2 + 4H_2O \qquad \text{(I-1)}$$

$$2NaAlO_2 + 4H_2O \xrightarrow{\text{Precipitation}} Al_2O_3 \cdot 3H_2O + 2NaOH \qquad \text{(I-2)}$$

$$Al_2O_3 \cdot 3H_2O \xrightarrow{\text{Dehydration}} Al_2O_3 + 3H_2O \qquad \text{(I-3)}$$

The object of the precipitation step is to obtain maximum production

of correctly sized alumina trihydrate crystals while operating under economically feasible conditions. To do so requires a thorough understanding not only of the mechanisms involved but also of the effects of a multitude of factors upon these mechanisms. Many aspects of this crystallization process have received extensive study and are well understood. For example, the effects of variables such as caustic and alumina concentrations, temperature, and seed charges have been thoroughly investigated.[13,14,21] Also, the properties of sodium aluminate solutions---viscosity, osmotic character, electrical conductance, structure of the aluminate ion, etc.---have received considerable attention.[21] However, there still exists one important area of study where very little work has been performed, i.e., the study of the effects of various impurities and constituents upon the crystallization process.

One outstanding characteristic of typical Bayer plant liquor is that it contains a large number of components over and above the necessary sodium hydroxide, sodium aluminate, and alumina hydrate. Many of these components enter the plant stream with the bauxite (see Table I). Others are intentionally added to the plant stream to improve operations, e.g., starch and lime to facilitate clarification of the digestion effluent. Regardless of their origins these constituents, in many cases, influence various phases of the Bayer process. The extent of these influences upon the crystallization step in particular may range from negligible to highly significant. An understanding of these influences and the mechanisms by which they operate would render possible a more efficient and profitable operation. To date, only a few of the many impurities and constituents present in Bayer liquors have been studied

TABLE I

ANALYSIS OF A TYPICAL BAUXITE

Component	Weight %
Al_2O_3	55.460
SiO_2	2.350
Fe_2O_3	11.710
TiO_2	.680
MnO	.010
CaO	.120
MgO	.400
Cr_2O_3	.003
CuO	.004
K_2O	.012
Li_2O	.020
MoO_3	.003
Na_2O	.013
PbO	.002
P_2O_5	.025
V_2O_5	.002
Loss on ignition	29.186
	100.000

with respect to their effects upon the crystallization of alumina trihydrate. This research was undertaken to determine and define the influences upon the crystallization step exerted by several such constituents. A secondary purpose of this study was to develop the apparatus necessary to accomplish this investigation.

A survey of the technical literature pertinent to sodium aluminate solutions and to the crystallization of alumina trihydrate therefrom yielded very little concerning the effects of impurities upon the crystallization step. (Throughout the remainder of this paper all constituents other than sodium hydroxide, sodium aluminate, aluminum hydroxide, alumina hydrate, and water will be referred to as impurities.) Pearson[21] briefly mentions several impurities suspected to act as crystallization "poisons" but presents, and refers to, no experimental evidence. Ivekovic et al[9] studied the crystallization of alumina trihydrate from sodium aluminate solutions containing various alcohols and starch. Sato[23] investigated the influences of starch, glucose and sugar on the crystallization process. No other references to studies of the effects of impurities in sodium aluminate solutions were found. Since this left a myriad of choices as to possible subjects for investigation, a decision was made to study the influences of three particular impurities upon the Bayer crystallization step. The impurities chosen were:

1. sodium oxalate, $Na_2C_2O_4$
2. starch, $(C_6H_{10}O_5)n$
3. magnesium

The reasons for these choices are discussed in Chapter II.

It was decided to study the effects of each of these impurities individually in an otherwise pure sodium aluminate solution. In actual Bayer plant liquors the possibility exists for interactions between pairs, or all, of these impurities to produce effects on the crystallization step that can not be predicted from studies of the individual effects. However, studies of the effects of single impurities are certainly justifiable as a starting point, and may serve as guides to subsequent investigations of more complex systems.

An experimental technique for obtaining the necessary data was required. The literature survey yielded information that served as the basis for the final choice of an experimental apparatus. Reported in various forms by Pearson,[21] Joseph,[10] and Kuznetsov[13] was the fact that the electrical conductance of a sodium aluminate solution increases appreciably as the crystallization of alumina trihydrate from that solution proceeds. Accordingly, it was decided to assemble an apparatus that would exploit this feature in following the crystallization process. This equipment is discussed in Chapter III.

In summation, this research has as its goal the determination of the effects of three specific singly acting impurities upon the crystallization of alumina trihydrate from a pure sodium aluminate solution. In conjunction with this goal, an experimental apparatus to procure the necessary data was designed and assembled. It is hoped that this study, along with subsequent studies of a similar nature, will eventually lead to a complete theoretical understanding of the Bayer crystallization mechanism, which, in turn, will result in an improved process for the production of alumina.

CHAPTER II

THEORY

1. Theory of Crystallization[20,22,26]

In general the process of obtaining crystals from a solution involves two separate, but often simultaneous, mechanisms: first, the formation of new crystals, or nucleation, and second, the growth of existing crystals. In order for either of these actions to occur, there must exist a state of unbalance with a decrease in chemical potential between the bulk of the solution and the crystalline surface. This means that the solution must be supersaturated.

A convenient, but oversimplified, explanation of the competition between these mechanisms was offered by Miers[17] when he postulated that the region of supersaturation can be divided into two parts, labile and metastable, with the line of demarcation being the supersolubility curve (see Figure 1). According to this theory, crystal growth occurs only when the concentration of the solution lies above the saturation curve, A, and nucleation is possible only in the labile region. In other words, referring to Figure 1, any point, F, below the saturation curve is unsaturated and will not promote or yield crystalline material. A point, D, in the metastable region will promote crystal growth and will drop to concentration E if seed is added, but will remain unchanged at D if no such seed crystals are present. Concentrations above the supersaturation curve, such as point C, will spontaneously crystallize

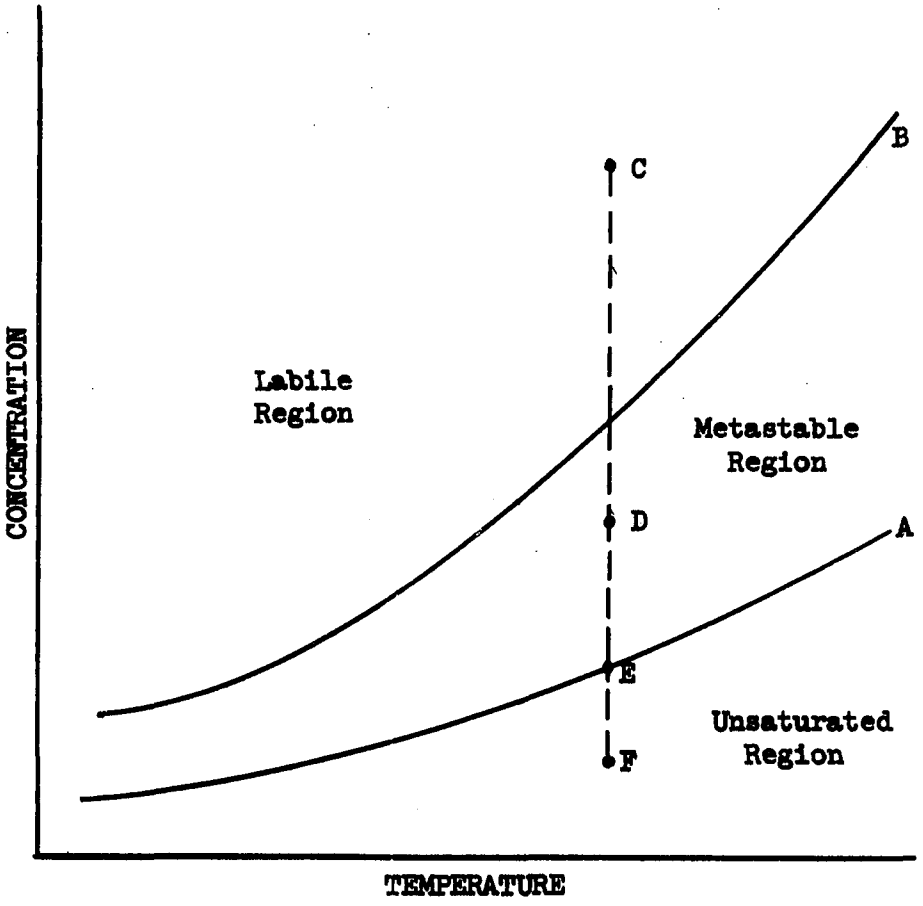

Figure 1. Miers Solubility Diagram

A - Saturation curve
B - Supersaturation curve

to ultimately yield concentration E by both nucleation and growth mechanisms. In those cases where Miers' theory holds, the relative rates of nucleation and growth are readily controlled. This is accomplished by adjusting the concentration of the solution to either the labile or metastable zone to render the desired effects. Unfortunately, attempts to establish well-defined supersolubility curves for many solutions, including sodium aluminate solutions, have generally been unsuccessful, and the existence of such curves for these solutions is doubtful. Therefore, a sounder, more comprehensive discussion must be considered.

Van Hook[26] presents such a discussion in his third chapter, titled Modern Theories. Crystallization is pictured as a probability function having two somewhat similar mechanisms. The first mechanism, nucleation, is based on the probability of the required number of particles (atoms or molecules) coming together simultaneously in the requisite geometrical arrangement to form a nucleus. To form such a new phase, an energy barrier particular to the mother phase and the nucleus must be surmounted. Once such nuclei are present, the second mechanism, crystal growth, becomes significant. This mechanism is a function of the probability of the appropriate material being transferred from the liquid bulk to the solid-liquid interface and then being incorporated into the crystal lattice. It is intuitively obvious that the greater the degree of supersaturation, the greater will be the probabilities for these mechanisms to successfully occur.

Historically, the nucleation and growth mechanisms were considered to be mutually independent with the former being the slower and more difficult. This distinction may be qualitatively verified, to a reason-

able degree of satisfaction, from an examination of the kinetics represented by Eyring's activated complex theory,

$$k = \frac{RT}{Nh} \quad \frac{\Delta S^*}{R} \quad \frac{-\Delta H^*}{RT} \qquad \text{(II-1)}$$

where k is the specific reaction rate constant, R the gas constant, N Avogadro's number, h Planck's constant, and ΔS^* and ΔH^* are the entropy and enthalpy of activation. Van Hook asserts that it is reasonable to expect ΔH^* to be of the same order of magnitude for both the nucleation and growth mechanisms. However, the entropy change involved in forming the initial nucleus should be much greater than for the addition of further particles to an already existing and ordered base. Consequently, since entropies of crystallization are inherently negative, the nucleation rate constant will be smaller than the growth rate constant. The actual difference in these constants depends, of course, on the relative magnitudes of the entropies and enthalpies of activation.

The interrelationship between the nucleation and growth processes was generally overlooked by most of the early workers until, as Van Hook mentions,[1] Kossel's proposed mechanism of crystal growth. Prior to Kossel most of the experimental studies dealt with either nucleation or growth independently. Kossel's model is schematically represented in Figure 2. Kossel theorized that crystal growth consists of the deposition, unit by unit, of successive strips, such as strip A-B, with these strips advancing across the uncompleted layer. This will continue

---

[1] See Van Hook's Chapter III, bibliography.

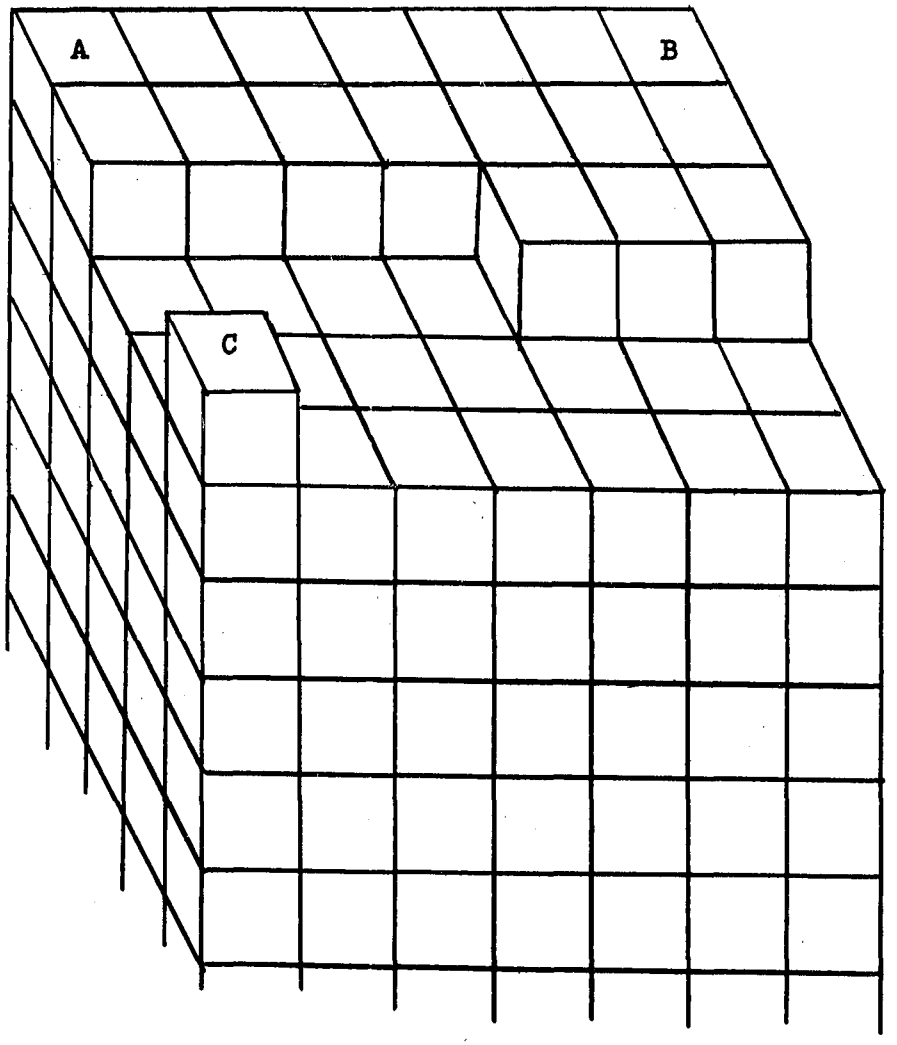

Figure 2. Kossel's Crystal Model

until that particular layer is completed. For crystal growth to continue, a new layer (step) must be originated. This is accomplished by a process of two-dimensional surface nucleation which provides a base for continued growth on a new plane. (A two-dimensional nucleus is represented by C in Figure 2.) Thus, Kossel's mechanism of crystal growth is analogous to the process of writing a book, i.e., the subsequent addition of new characters to each line, of new lines to each page, and a transition to a new blank page after the preceding one has been filled. A number of refinements have been incorporated into the theory by Volmer, Stranski and others, but in this paper, the discussion of these refinements is unwarranted.[2] It is sufficient to indicate that this model suggests the unification of nucleation and growth ideas, since the growth of a particular crystal surface will be a function of the probability of surface nucleation, the step height, and the rate of advance of the step.

Numerous experimental studies have demonstrated the validity of Kossel's model and the reality of two-dimensional nucleation for many systems.[3] Yet, for other systems, tremendous discrepancies were observed between theory and experiment. It should be apparent from the foregoing general discussion of Kossel's model that delays in growth are expected whenever a surface layer is completed and a new step must be initiated. This is due to the slowness of the nucleation process relative to the

---

[2] Ibid.

[3] Ibid.

growth process. However, many systems exhibit no such delays. This incongruity was finally rationalized by F. C. Frank at the Bristol Symposium on Crystal Growth in 1949.(4) Frank postulated that the necessity for surface nucleation is obviated if the crystal contains a self-perpetuating dislocation. Such a dislocation essentially causes the crystal surface to resemble a helical ramp arranged in the direction of a right- or left-handed screw. Thus, after completing one entire layer, the dislocation still exists, but one layer higher. Since a step is consequently always present on the crystal surface, there is no longer any need for two-dimensional nucleation, and so the expected delays in growth due to nucleation are absent ipso facto. As a result of Frank's proposal, an extensive search for growth spirals was made and, in many cases, such spirals were found.[4] On the basis of this evidence, Frank's dislocation mechanism appears to be very much a reality.

The preceding discussion presents a simplified description of the two accepted models for crystal growth---Kossel's and Frank's. Nothing has yet been mentioned of the restrictions that may apply to these models. As in the case of any heterogeneous reaction, certain consecutive requirements must be met. These are, in order:

1. Transport of reactants from liquid bulk to the solid-liquid interface
2. Adsorption on crystal surface
3. Orientation in the surface
4. Desorption of products from surface
5. Transport of products from interface to the liquid bulk

---

[4] Ibid.

Should any one of these consecutive steps be much slower than the others, the over-all rate of growth will occur at approximately that velocity. Hence, a number of factors exist that may significantly affect crystal growth.

In this study it is believed that experimental conditions were so adjusted that the first and last of the five steps outlined above are negligible. This effect was achieved by subjecting the crystallizing system to vigorous agitation---approximately 1500 rpm. (For details of the apparatus refer to Chapter III.) It was visually apparent that good suspension and dispersion were obtained throughout all experimental runs. Pearson,[21] commenting on the effects of agitation upon the crystallization of alumina trihydrate, asserts "The rate of decomposition thus increases with stirring rate until the seed is completely dispersed. It then remains virtually constant until the stirring becomes so vigorous that fresh particles are formed through attrition." On the basis of this and actual observation, resistance to mass transfer to and from the interface is assumed negligible.

The fourth step, desorption of products from the crystalline surface, may also be discarded. In phase transitions this consists essentially of the dissipation of the latent heat of transition. Van Hook[26] maintains that this is unimportant except for extremely rapid rates of growth. As observed experimentally, alumina trihydrate crystallizes at a moderately slow pace, so no significant temperature gradients across the solid-liquid interface are expected. Also, the vigorous agitation already mentioned should aid in the dissipation of the heat of transition.

By process of elimination, the adsorption and surface orientation

steps must then be the rate-determining factors. Any variable that favors adsorption and orientation of the appropriate material will increase the rate of crystal growth; conversely, any obstruction of adsorption or orientation will inhibit crystal growth. The aim of this study is to determine the effects of various impurities (sodium oxalate, starch, magnesium) in the crystallizing system upon these two critical steps, adsorption and orientation.

2. Sodium Aluminate Solutions and the Crystallization of Alumina Trihydrate

An understanding of the alumina trihydrate crystallization process requires a knowledge of the nature of sodium aluminate solutions. Pearson provides a comprehensive review of the experimental studies pertinent to these solutions.(21) As Pearson points out, it is impossible to prepare a solution of pure sodium aluminate free from excess caustic soda. In other words, the mole ratio of Na_2O/Al_2O_3[5] in solution must always exceed unity. As this ratio approaches unity, the solution becomes very unstable and decomposes to the trihydrate and caustic soda. Consequently, as it is impossible to obtain or isolate pure sodium aluminate, the study of this compound is difficult. However, it is possible to formulate a description of this compound on the basis of studies made of its solutions. Any acceptable description of sodium aluminate must be compatible with the experimental findings summarized by Pearson:

a) Osmotic properties -- The freezing-point depressions and boiling-

---

[5] See Appendix A -- Nomenclature.

point elevations of aqueous caustic soda solutions of varying concentrations are unchanged by the dissolution of alumina therein. These identical osmotic properties of sodium aluminate and sodium hydroxide solutions indicate that both contain the same number of ions, i.e., that a structure such as sodium ortho-aluminate, Na_3AlO_3, which yields four ions per molecule,

$$Na_3AlO_3 \longrightarrow 3Na^+ + AlO_3^{-3}$$

is an unsuitable model for sodium aluminate.

b) Electrical conductance -- An appreciable increase in equivalent conductance is noted when sodium aluminate solutions decompose to yield alumina trihydrate and sodium hydroxide. From the data of Joseph,[10] Kuznetsov,[13] and Pearson,[21] it is evident that the mobility of the aluminate ion, whatever its structure, is considerably less than that of the hydroxide ion. As mentioned in the previous chapter, this study uses this characteristic to follow the progress of the crystallization process. For an illustration of the suitability of this technique, refer to Figure 3, which is taken from Kuznetsov.[13] However, it must not be assumed that, as a sodium aluminate solution isothermally decomposes, the per cent increase in conductance equals the per cent decrease in dissolved aluminum. This is because the change in conductance depends on two ions: aluminate and hydroxide. As decomposition proceeds, the action of a single aluminate ion yielding a hydroxide ion has a continuously smaller and smaller influence on the solution's electrical conductance. In other words, the change in conductance versus the degree of aluminate decomposition is <u>not</u> linear. On the other hand, the

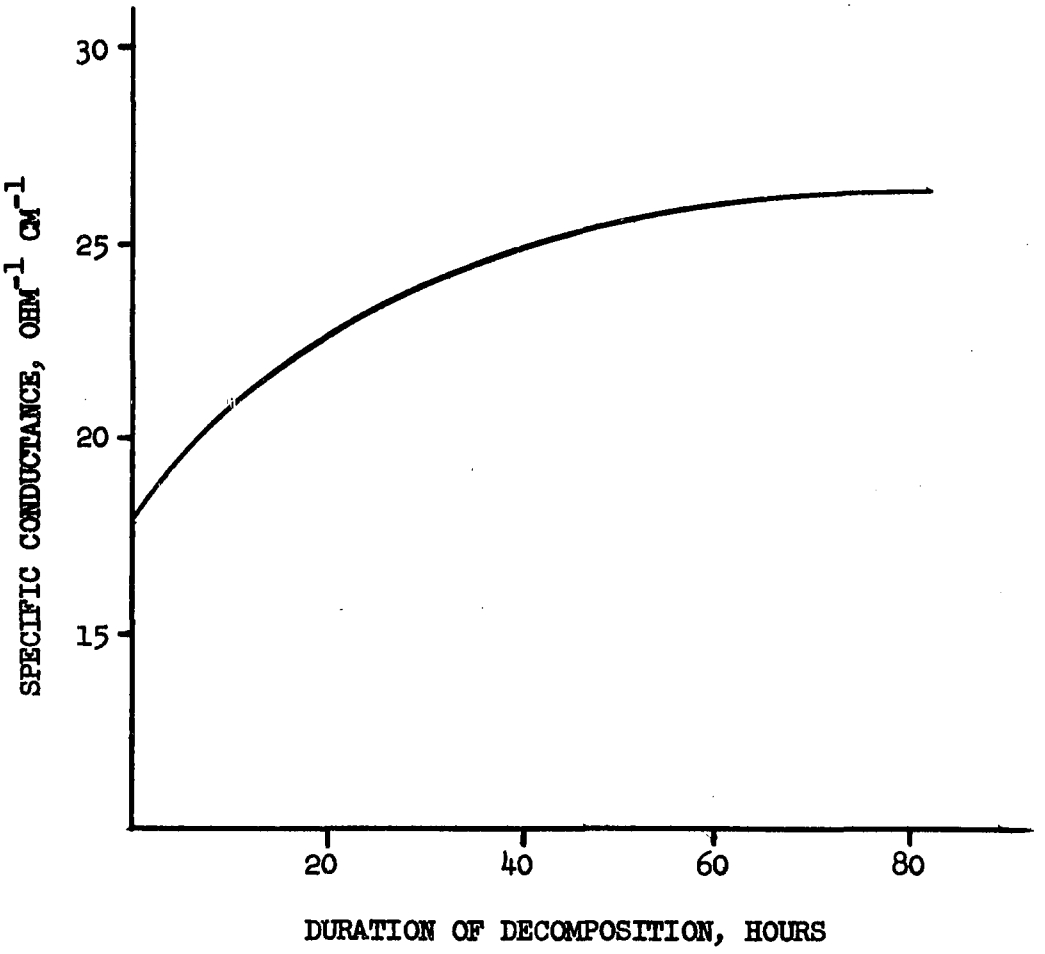

Figure 3. Variation of Specific Conductance of a Sodium Aluminate Solution During Decompositon. T = 30°C. Original solution: $Na_2O_{tot.}$ = 130 gpl, $Na_2O_{caustic}/Al_2O_3$ = 1.6, Seed ratio = 1.0.

dissolved aluminum concentration versus the degree of aluminate decomposition is linear. Therefore, a per cent change in conductance must not be equated to the same numerical per cent change in dissolved alumina.

c) Viscosity -- The dissolution of alumina in a caustic soda solution results in a great increase in the solution's viscosity. For example, the viscosity of a 10M NaOH solution at 25°C is 10.4 centipoises. The dissolution of 3.97 moles of Al_2O_3 in this 10M solution causes the viscosity to increase to approximately 600 centipoises.

d) Hydrogen electrode measurements -- Direct comparisons between hydrogen electrodes in caustic soda solutions and sodium aluminate solutions of the same molarity indicate that, over a wide range of concentrations, the degree of hydrolysis is 10 per cent or less.

This experimental evidence can be analyzed for the insight it may provide as to the structure of sodium aluminate. First, as already pointed out, the osmotic properties indicate sodium aluminate to be a uni-univalent molecule. Also, the osmotic properties plus the high viscosities of sodium aluminate solutions suggest the complete hydrolysis of these solutions to give heavily-hydrated colloidally-dispersed aluminum hydroxide, i.e.,

$$\text{Na aluminate} + H_2O \longrightarrow Na^+ + OH^- + \underset{\text{colloidal}}{Al(OH)_3(H_2O)_3}$$

However, this model of complete hydrolysis conflicts with the results of hydrogen electrode and electrical conductance measurements. Therefore, another explanation must be sought. The high viscosities may be attributed to heavy hydration of the aluminate ion. Such a model is

consistent with the other aforementioned properties of sodium aluminate solutions. Further justification of this model is found in the tendency of the aluminum ion to add donor groups to satisfy its secondary valence.[2,18,21,28] Thus, the aluminate ion is pictured as a Werner complex with a primary valence of +3 and a secondary valence, or coordination number, of six (6). It can be envisaged as a small central aluminum ion in octahedral coordination with four hydroxyl ions and two water molecules, the net charge being one negative unit, i.e., $Al(OH)_4(H_2O)_2^{-1}$ (see Figure 4). The high viscosities of sodium aluminate solutions are thus accounted for by the linking of the hydrated aluminate ions with each other and with water by hydrogen bonding. Although this model is not known with certainty to accurately represent the aluminate ion, it is currently accepted as the most probable structure.

In Equations I-1,-2, sodium aluminate is represented by the formula, $NaAlO_2$. This is commonly done for convenience throughout the Bayer industry and its literature. It should be noted that the two formulas for sodium aluminate are essentially equivalent,

$$NaAl(OH)_4(H_2O)_2 \rightleftharpoons NaAlO_2 + 4H_2O$$

differing only in the disposition of the water molecules. Using the complex formula for sodium aluminate, Equations I-1,-2 may be rewritten as follows:

$$Al_2O_3 \cdot 3H_2O + 2NaOH + 4H_2O \xrightarrow{\text{Digestion}} 2NaAl(OH)_4(H_2O)_2 \qquad \text{(II-2)}$$

$$2NaAl(OH)_4(H_2O)_2 \xrightarrow{\text{Pcptn}} Al_2O_3 \cdot 3H_2O + 2NaOH + 4H_2O \qquad \text{(II-3)}$$

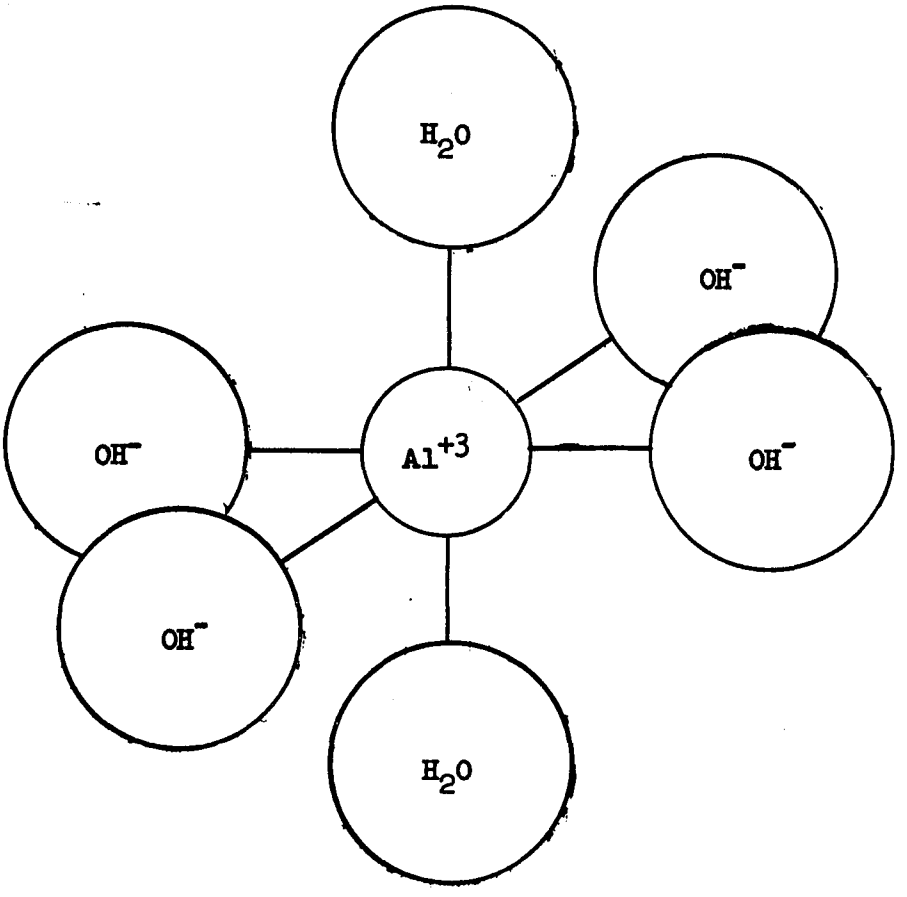

Figure 4. Model of Aluminate Ion. A Werner complex with coordination number of six (6).

At this point a more thorough discussion of the precipitation step, Equation II-3, is necessary. A number of authors[2,12,18,21,28] note that sodium aluminate solutions do not decompose directly to the crystalline trihydrate as indicated by Equation II-3 (I-2). Pearson states that freshly precipitated hydrated alumina tends to be gelatinous, but will be transformed to crystalline hydrate if stirred with crystalline seed hydrate.[21] Moeller asserts that the freshly precipitated material is amorphous but that upon aging it becomes crystalline.[18] According to Kolthoff and Sandell,[12] an amorphous primary precipitate, such as hydrous aluminum oxide,[6] ages at higher temperatures to yield a crystalline modification, the process being accompanied by a decrease in the total surface. Moreover, an aging due to chemical interaction between particles may occur, such as bridgings by hydroxyl and hydrogen bonds.[2,12,19] Consequently, although Equation II-3 is frequently used to represent the precipitation step, it appears that sodium aluminate actually decomposes to an amorphous primary precipitate which subsequently is converted to the crystalline trihydrate. Pearson suggests the following consecutive reactions:

$$NaAl(OH)_4\cdot(H_2O)_2 + H_2O \rightleftharpoons Na^+ + OH^- + \underset{\text{colloidal}}{Al(OH)_3\cdot(H_2O)_3}$$

$$\underset{\text{colloidal}}{2Al(OH)_3\cdot(H_2O)_3} \rightleftharpoons \underset{\text{crystalline}}{Al_2O_3\cdot 3H_2O} + 6H_2O$$

Using these suggested reactions the digestion-precipitation steps of

---

[6] See Appendix E.

the Bayer process are summarized below:

$$Al_2O_3 \cdot 3H_2O + 2NaOH + 6H_2O \xrightarrow{\text{Digestion}} 2NaAl(OH)_4(H_2O)_2 + 2H_2O \qquad (II\text{-}4)$$

$$2NaAl(OH)_4(H_2O)_2 + 2H_2O \xrightarrow{\text{Precipitation}} \underset{\text{colloidal}}{2Al(OH)_3 \cdot (H_2O)_3} + 2NaOH \qquad (II\text{-}5)$$

$$\underset{\text{colloidal}}{2Al(OH)_3 \cdot (H_2O)_3} + 2NaOH \xrightarrow{\text{Crystallization}} \underset{\text{crystalline}}{Al_2O_3 \cdot 3H_2O} + 2NaOH + 6H_2O \qquad (II\text{-}6)$$

Considering Equation II-6, little is known of the actual mechanism of this conversion step. A general discussion of conversions of this type is found in Dean's text on colloids.[2] In the case of $Fe(OH)_3(H_2O)_3$, Dean proposes that this uncharged molecule is unstable and immediately polymerizes with loss of water. An analogous reaction is shown for colloidal $Al(OH)_3 \cdot (H_2O)_3$ below:

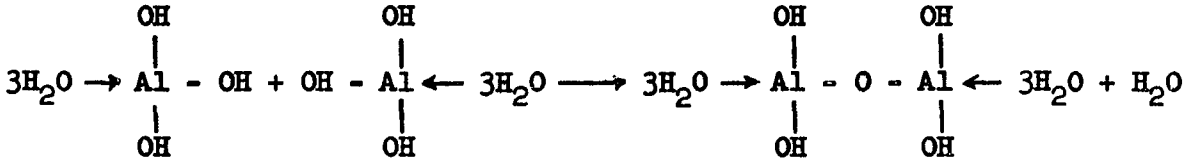

Such a polymerization can be extended to result in colloidal structures such as that of Figure 5, which is best represented by the formula, $Al_2O_3 \cdot xH_2O$. Two such neutral colloidal particles of $Al_2O_3 \cdot xH_2O$ are very likely to stick together if they come in contact. Water may be eliminated between OH groups on the surface atoms of Al, forming an oxygen bridge and thus joining the two particles. If several such bridges are formed between two particles, they will eventually become one. Since they initially stick together only at points of contact, a large amount of water is enmeshed in the

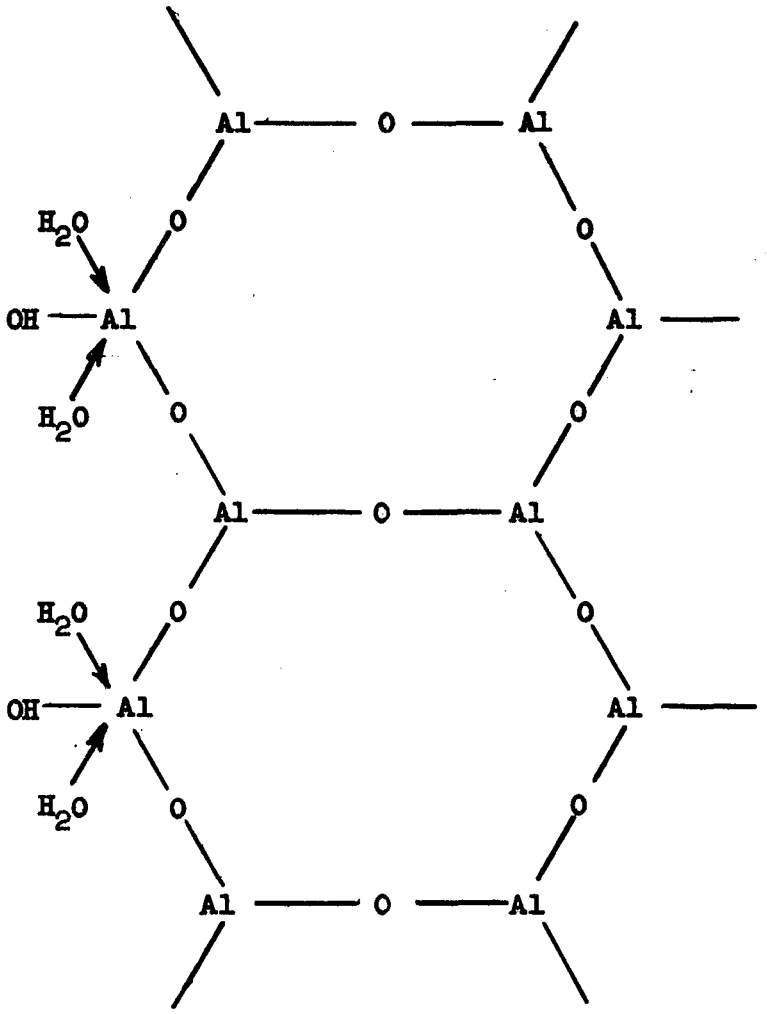

Figure 5. $Al_2O_3 \cdot xH_2O$

colloidal structure. As this structure ages, there will be a rearrangement of the atoms to yield a smaller total surface area. The result is a crystalline structure. This crystalline material, designated $Al_2O_3 \cdot 3H_2O$, gibbsite or hydrargillite, is built up of double layers of hydroxyl groups with aluminum atoms occupying two-thirds of the octahedral holes between the layers. Hydroxyl bonds hold the adjacent layers of OH groups together. Figure 6 presents a view of one face of the $Al_2O_3 \cdot 3H_2O$ crystal model. (Alcoa's Technical Paper No. 10[19] includes photographs of models of this crystal along with a fine discussion of the structure.)

From the preceding discussion and upon examination of Figure 6, it is apparent that no water of hydration is actually present in the crystalline material designated $Al_2O_3 \cdot 3H_2O$. As is the case with several other compounds encountered in the aluminum industry, the term alumina trihydrate, although now recognized as a misnomer, is still commonly used out of custom. Actually, a more correct name is alumina trihydroxide. However, the terminology of the aluminum industry has little to do with the nature of this study, so no more attention will be devoted to its explanation. Let it suffice to note that a summary of the various terms and designations may be found in Alcoa's publication[19] if further information on this subject is desired.

The important thing to understand from Equations II-5,-6 is that the crystallization of alumina trihydrate can be influenced in two major ways:

1. The conversion from the colloid to the crystalline material may be affected, and

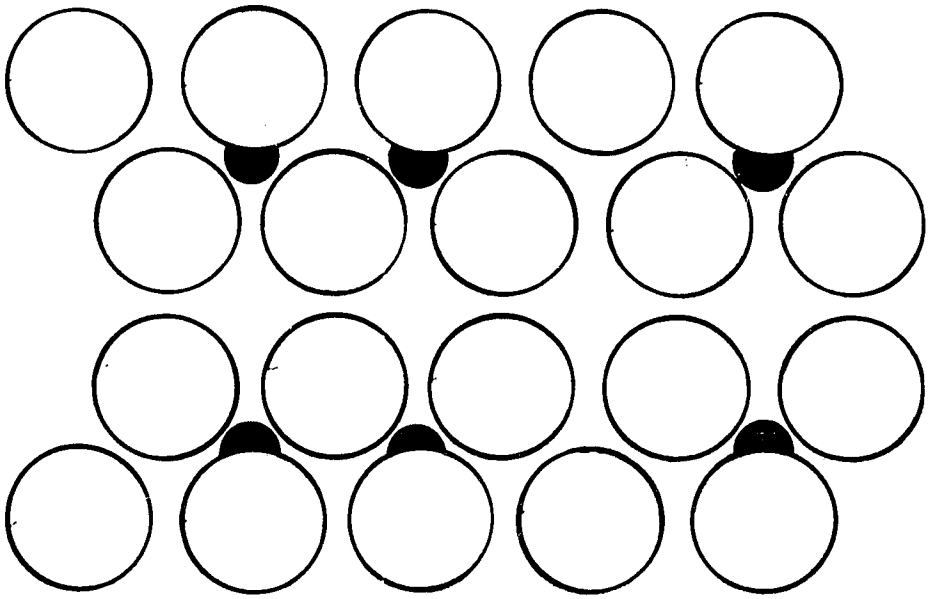

Figure 6. Model of $Al_2O_3 \cdot 3H_2O$ (Gibbsite). The blank circles represent OH^- ions. The dark half-hidden circles represent Al^{+3} ions.

2. The adsorption and surface orientation of new crystalline material by existing crystals may be affected.

Keeping these points in mind, let us now turn to a consideration of the impurities whose effects upon the crystallization step will be studied.

3. Impurities

Although it is possible that certain impurities will improve the crystallization of alumina trihydrate, this research was performed on the assumption that the added impurities would produce deleterious effects, i.e., that they would act as poisons. Poisons may affect the process broadly in three ways: a) by slowing it down over its entire course; b) by inhibiting it for a period; c) by inhibiting it indefinitely. A discussion of the actual poisoning mechanisms will be postponed until after the experimental results have been presented.

The three impurities chosen for investigation are, as listed in Chapter I, sodium oxalate, starch, and magnesium. The reasons for these choices follow:

a) Sodium oxalate, $Na_2C_2O_4$ -- An appreciable oxalate content is not uncommon in the liquor of many Bayer plants. In fact, several major aluminum companies are believed to have associated this oxalate with problems of product size in the precipitation process. The source of the oxalate is probably the degradation of various organics that enter the system via the bauxite or by addition of starch. No quantitative information concerning the effects of this impurity on the growth of alumina trihydrate crystals was found, although Pearson[21] does assert that sodium oxalate in the usual concentrations (5-10 gpl) of Bayer liquors has little effect. Consequently, since sodium oxalate is

present in appreciable quantities, and since it is suspected to influence some phases of the precipitation cycle, it was felt that a quantitative study of its effects upon the decomposition of sodium aluminate solutions was justified.

b) Starch, soluble, $(C_6H_{10}O_5)_n$ -- Most, if not all, Bayer plants add starch at some point in the process to aid in the clarification of the digester effluent. It is not improbable that appreciable solubilized starch reaches the precipitators, where it can influence the crystallization step. Ivekovic et al[9] studied the influence of starch upon the crystallization of the trihydrate and published the following results. Working with solutions containing approximately 1.49 moles/liter of Al_2O_3 and 2.2 moles/liter of Na_2O, the precipitation of alumina trihydrate was completely prevented by the addition of 6.7 gm/liter of starch. Sato,[23] on the other hand, implies that there is an optimum starch addition which will yield an accelerated decomposition of sodium aluminate, even when no crystalline seed is present. In view of this paucity of data, further study of starch additions was made in this research.

c) Magnesium, added as $4MgCO_3 \cdot Mg(OH)_2 \cdot 5H_2O$ -- According to Pearson,[21] magnesium occurs in bauxite in the range 0.05-0.4 per cent MgO, and although some of it finds its way into the liquor, the contribution from this source is not known to exercise any harmful effects on the Bayer process. However, Pearson asserts later that magnesium salts will very effectively poison trihydrate seed, yielding a marked induction period. On the basis of these comments it is thought that additional study of this impurity would provide a clearer picture of magnesium's effects upon the crystallization step. Since the actual magnesium

salts present in Bayer liquors are not known, the choice of the complex compound, $4MgCO_3 \cdot Mg(OH)_2 \cdot 5H_2O$, was arbitrarily made.

CHAPTER III

EXPERIMENTAL TECHNIQUES AND APPARATUS

1. General

After considering possible methods of studying the problem, it was decided to follow the course of the crystallization process by electrical conductance measurements. Equation II-5 indicates that every decomposing aluminate ion yields one hydroxide ion, so an appreciable increase in conductivity with decomposition is expected. This variation of conductivity with decomposition has already been demonstrated in Figure 3.

The advantage of this method is that it obviates the taking of incremental samples at varying time intervals for chemical analysis, thereby eliminating a large amount of analytical work. For instance, several of the experimental runs required conductance (or resistance) measurements every 15 minutes for the first two hours and every 30 minutes for the next six hours. This is a total of 20 measurements for the first eight hours of operation. A corresponding number of grab samples requiring chemical analysis would have presented an almost prohibitive quantity of work.

The choice of temperature conditions had to be resolved. Kuznetsov and coworkers[13,14] conducted most of their experimental work under conditions of gradual temperature decrease to simulate industrial practice. Typical temperature ranges were 75°-55°C and 61°-40°C. However, for the present study, the choice of non-isothermal operation was dis-

carded in favor of isothermal conditions for two reasons:

a) Kuznetsov[13] notes that the specific conductances of decomposing sodium aluminate solutions are essentially constant when the solutions are subjected to a gradual temperature decrease. This is because of two opposing factors: decomposition leads to an increase in conductance, whereas cooling causes the conductance to decrease. If both decomposition and cooling occur simultaneously, their effects on conductance tend to cancel one another, causing the conductance to remain virtually unchanged. This can be avoided by operating isothermally, thus rendering the conductance of a given solution a function of decomposition only.

b) Difficulty in obtaining reproducible cooling rates was anticipated. Such a problem is non-existent for isothermal conditions.

To approximate actual industrial temperatures the decision was made to conduct all runs at 70.0°C. Examination of experimental data (Appendix G) reveals that actual temperatures varied from 69.9-70.1°C for most of the runs.

Agitation within the crystallizing system is necessary for two reasons: first, to minimize temperature and concentration gradients, and second, to provide good dispersion of crystals so as to maximize crystal surface area available for crystal growth. To eliminate the degree of agitation as a variable, all runs were made under the same stirring conditions. This was accomplished by agitating with a variable speed mixer set to operate at approximately 1500 rpm. The mixer is described in Section III-6g. The setting, 1500 rpm, was determined to be satisfactory by trial-and-error.

2. Outline of Experimental Procedure and of Data to be Obtained

To investigate the effects of impurities on the crystallization process the following general procedure was employed for each experimental run:

a) Make up a batch of a standard supersaturated sodium aluminate solution. (See Section III-3.)

b) Put four liters of this standard solution into the crystallization vessel, immerse the vessel in an isothermal (70°C) oil bath, and allow the temperature of the contents to attain equilibrium. Agitate contents at 1500 rpm. (Section III-6 describes the equipment.)

c) Add a measured amount of impurity (Section III-4) to the standard solution in the crystallization vessel.

d) Add a known seed charge (Section III-5) to the contents of the crystallization vessel and begin taking resistance-vs-time readings.

e) When equilibrium of the crystallization process is indicated (i.e., when the resistance shows little or no variation with time), stop the experimental run; separate the crystals from the supernatant liquor by filtration.

f) Analyze the supernatant liquor for dissolved NaOH and Al_2O_3.[25]

g) Dry crystals in oven at 108°C for 24 hours.

h) Obtain sieve analysis of crystals. (See Section III-7f.)

i) If required, obtain a microphotograph of the crystals.

3. Standard Sodium Aluminate Solutions

To facilitate comparisons of the effects of different impurities

on the crystallization step, variations in the composition of the original pure sodium aluminate solutions must be minimized. This may be accomplished by conducting each of the experimental runs on the basis of a standard solution, to which the various impurity and seed charges are added.

Bayer plant liquor contains NaOH concentrations of 4-6 molar. These concentrations were considered too high for the purposes of this investigation for two reasons:

a) Using the resistance-measuring equipment available, industrial caustic concentrations resulted in resistance readings beyond the instrument's range. It was not possible to remedy this by modifying the cell constant, since such modifications resulted in impractical electrodes.

b) Previous workers,[14,23] in studying the crystallization process in liquors of Bayer plant concentrations, have used glass vessels to contain the solutions. Even at these relatively high concentrations, none reports any reaction between the solutions and the glass walls of the vessels. To minimize the possibility for such a reaction to occur to any appreciable extent, it was decided to use caustic solutions of much weaker concentrations than actual Bayer liquors.

Consequently, the standard sodium aluminate solution used for all experimental runs is made up in the following manner. To 4 liters of distilled water add 160 grams of reagent grade NaOH. This yields a 4-liter (approximately) solution of 1-molar NaOH. To this, add pure aluminum (99.99% Al) in the proportion, 16.2 grams of aluminum per liter. An exothermic reaction results upon the addition of aluminum to a sodium hydroxide solution according to the equation

$$Al + NaOH + 5H_2O \longrightarrow NaAl(OH)_4(H_2O)_2 + 1^{1/2}H_2 \uparrow$$

liberating hydrogen as indicated. A solution containing the above proportions of aluminum and sodium hydroxide is very supersaturated at 70°C, as is seen from Pearson's[21] Figure 6, and decomposes readily in the presence of seed. However, if no seed is present, such a solution will remain virtually unchanged for a relatively long time.

4. Impurity Charges

Each of the impurities studied---sodium oxalate, starch, and magnesium---was treated in a different way. Thus, it is more convenient to discuss each impurity separately.

a) Sodium oxalate, $Na_2C_2O_4$ -- All oxalate runs were made with oxalate charges of .05 moles of $Na_2C_2O_4$ per mole of dissolved Al_2O_3. This is approximately equivalent to industrial $Na_2C_2O_4/Al_2O_3$ ratios. Actual oxalate concentrations in the experimental runs were about 2.0 gpl. All oxalate charges were completely soluble.

b) Starch, soluble, $(C_6H_{10}O_5)_n$ -- Soluble starch is a white, odorless, tasteless powder that is soluble in water. It is essentially amylodextrin. Chemically, amylodextrin is a chain of approximately 25 glucose residues linked with typical starch unions and containing very little or no branching. A number of different starches are used in industrial practice, such as potato, corn, tapioca, etc.

The experimental starch concentrations varied from .025-5.0 gpl. Starch concentrations in the precipitation step of actual Bayer plants are unknown. For each experimental starch run, the starch was added to the standard solution only after the solution had attained a temperature

of 70.0°C. The starch was allowed to "cook" 30 minutes at this temperature before the seed charge was made.

c) Magnesium, added as $4MgCO_3 \cdot Mg(OH)_2 \cdot 5H_2O$ -- Different additions of this compound, basic magnesium carbonate, were made, resulting in concentrations ranging from .025 to .75 gpl. Solubility data for this compound is scarce. The Merck Chemical Index reports that it is soluble in CO_2-free water in the ratio 1/3300 parts, and is more soluble in water containing CO_2. Solubility data for alkaline solutions was not found.

5. Seed Charges

Four different seed charges were used in conjunction with each of the three impurities. The four basic charges were:

a) Light charge of coarse seed, designated LC, 18.7 gm

b) Light charge of fine seed, designated LF, 18.7 gm

c) Heavy charge of coarse seed, designated HC, 93.5 gm

d) Heavy charge of fine seed, designated HF, 93.5 gm.

The seed used was $Al_2O_3 \cdot 3H_2O$ obtained from Kaiser Aluminum's Baton Rouge Works. Chemical analyses, sizes, and specific surface areas of the coarse and fine seeds were provided by Kaiser Aluminum and are found in Appendix D. A light charge consisted of .1 mole of trihydrate seed per mole of alumina dissolved in the standard solution. A heavy charge represented a seed-to-dissolved alumina ratio of 0.5. For comparative purposes, industrial seed charges have a ratio of approximately unity. Using the specific surface area information provided by Kaiser Aluminum, the basic seed charges furnish initial total areas available for crystal growth as follows:

a) Light coarse (LC) charge - 7,330 cm^2

b) Light fine (LF) charge - 24,300 cm^2

c) Heavy coarse (HC) charge - 36,600 cm^2

d) Heavy fine (HF) charge - 121,500 cm^2

As already indicated, each of these charges was dispersed in a volume of four liters of sodium aluminate solution (along with the impurity to be investigated).

6. Experimental Apparatus

The overall program having been outlined, it was necessary to design and assemble an apparatus capable of carrying out the procedure indicated in Section III-2. A survey of the literature pertinent to conductometric studies[3,12,13,14,20,22] proved to be of little help in the choice of equipment to be used, so the final design had to be determined from a trial-and-error approach.

Preliminary studies using commercial conductance cells[3] with concentrated sodium aluminate solutions (approximately 4 M NaOH) indicated the unsuitability of such cells. These preliminary studies also suggested the use of weaker concentrations in the sodium aluminate solutions to be investigated. After numerous modifications, a satisfactory cell was obtained. It will be discussed later.

It was initially proposed to conduct the crystallization reactions in a hemispherical stainless steel vessel. This vessel was to be surrounded, and thermally controlled, by a water-jacket through which water would continuously be pumped from, and returned to, an isothermal (70°C) reservoir. A pair of electrodes and an agitator were to be provided for the crystallization vessel. For various mechanical reasons this proposal

was rejected in favor of a simpler design.

Numerous modifications and innovations followed. They finally resulted in a satisfactory apparatus, the essential elements of which are listed below along with a brief description of their functions.

a) Crystallization vessel -- A 5-liter 3-neck glass distilling flask (Pyrex #4960). An agitator is mounted through the large central neck and two platinum electrodes through the two smaller necks. The vessel is air-tight because the agitator shaft enters via a mercury-seal joint and the electrodes are mounted in ground-glass joints. Suppcrt for the crystallization vessel is provided by a bearing ring which rests on the floor of the isothermal reservoir. See Figure 7.

b) Isothermal reservoir -- The crystallization vessel is almost completely submerged in an oil bath (only the necks protrude above the surface of the reservoir's liquid). The purpose of this oil bath is to provide an isothermal environment for the crystallization vessel and its contents. The reservoir, itself, is a box-shaped container having no top with dimensions of 14" x 18" x 14". It has an outside 1" coating of asbestos insulation to minimize heat losses. The reservoir is filled approximately half-way with SAE 20 motor oil. To provide temperature control, a 500-watt heater and a resistance bulb thermometer are immersed in the oil. An agitator is mounted to provide adequate mixing and thus preclude temperature gradients within the bath. A copper cooling-coil (for carrying tap-water) lines the inside walls of the reservoir to provide for rapid cooling of the bath.

c) Temperature controller, Hallikainen Instruments "Resistotrol" -- This instrument turns the 500-watt reservoir heater off or on depend-

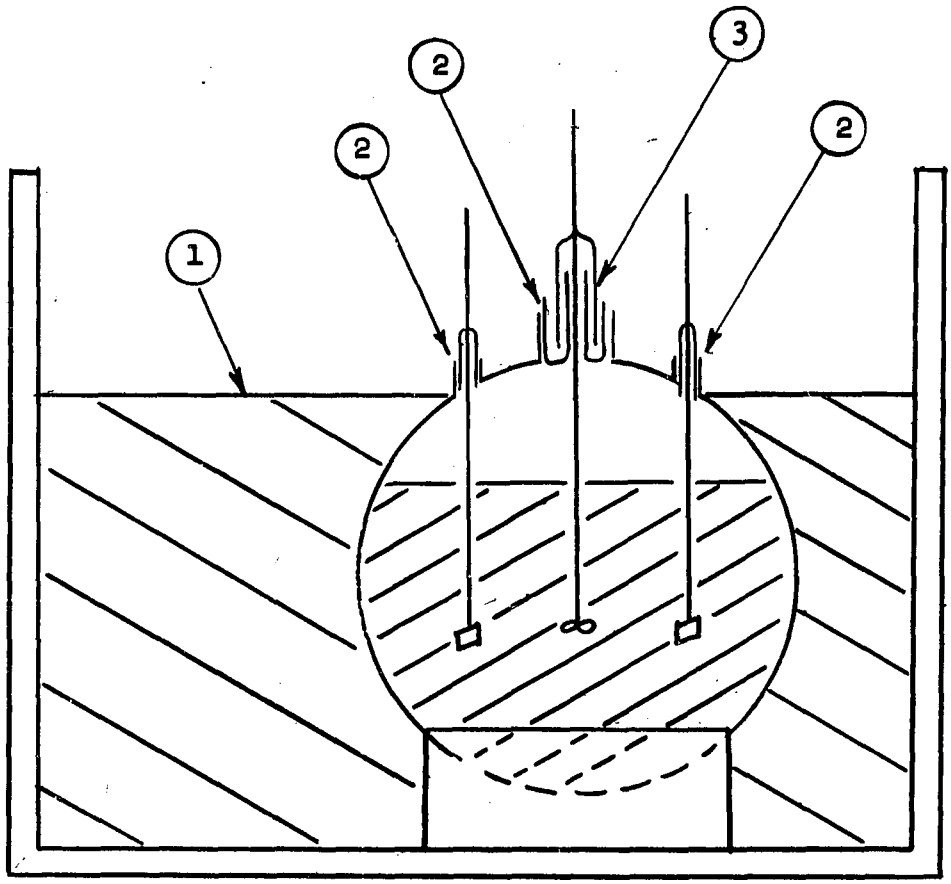

Figure 7. Crystallization Apparatus

(1) Oil Bath
(2) Ground Glass Joint
(3) Mercury Seal

ing upon whether the immersed resistance-bulb thermometer indicates a high or low temperature. The resistance-bulb thermometer is an integral part of the controller. With this apparatus the temperature of the contents of the crystallization vessel is readily maintained within $\pm 0.1^{\circ}C$ of the desired temperature.

d) Platinum electrodes (2) -- Each electrode plate is approximately 1 cm. square and is attached to a platinum wire stem about 12" long. This platinum stem is enclosed in a glass shield (Pyrex tubing) which is sealed around the wire just above the electrode plate. The glass shield is long enough (about 9") to allow the complete immersion of the electrode's surface in the contents of the crystallization vessel. The electrodes are mounted in the crystallization vessel via ground-glass fittings. When platinized and in place, the pair of electrodes comprise a conductance cell with a cell constant[1] of approximately 0.376 cm^{-1}. The external ends of the platinum wire stems are connected by copper leads to the conductivity bridge.

e) Conductivity bridge, Industrial Instruments, Inc., Model RC-1C -- This instrument is calibrated in ohms of measured resistance, covering the range of 0.2-2,500,000 ohms, with an effective accuracy of $\pm 1\%$ of the scale reading. Operating on 60 cps power, this model incorporates a vacuum tube oscillator circuit which supplies a 1000 cps bridge current. Used in conjunction with the previously described electrodes, this conductivity bridge measures the changing resistance of the decomposing sodium aluminate solutions.

---

[1] See Appendix B.

f) Variable Laboratory Capacitor, Westinghouse Electric Corp. -- Provides capacitance varying from 1/2 to 31 1/2 microfarads. The use of an external capacitance with the aforementioned conductivity bridge is necessary when measuring low resistance solutions so that a satisfactory null balance indication may be obtained.

g) Variable speed agitators (2), Lightnin Model F Mixer -- One provides circulation for the oil bath. The second agitator, equipped with a stainless-steel shaft and propellor, is set to rotate at 1500 rpm within the crystallization vessel. The shaft is 12" long, 1/4" in diameter, and is equipped with a two-bladed helical propellor, the tip-to-tip diameter of which is 2". The speed range of the agitators is 0-2000 rpm.

7. Miscellaneous

A number of minor points concerning procedure are worthy of mention.

a) As each new modification of the apparatus was assembled, a trial run was made with a sodium aluminate solution. The purpose of this trial run was to check out the reproducibility and reliability of the equipment. The run consisted merely of heating the solution gradually to about 90°C and then allowing it to cool, resistance-vs-temperature readings being taken for both heating and cooling legs of the run. These trial runs on the earlier versions of the apparatus resulted in the many modifications leading to the final design which performed satisfactorily.

b) In the course of the preliminary trial runs it was found that irregular and worthless data would result from continuous immersion of the electrodes in the decomposing solution. This is because of the gradual deposition of the trihydrate on the electrode plates, thereby

causing a change in the cell constant. To prevent this, the electrodes were suspended in distilled water between readings and were immersed only for the short time necessary to take the resistance readings. During the interims the two small necks of the crystallization vessel were stoppered to prevent an appreciable carbonation of the solution by the atmosphere. Between runs the cell constant was checked (see Appendix B). If a significant increase in cell constant was noted, the electrodes were cleaned and replatinized.

c) A line resistance of 1.25 ohms was placed in the bridge circuit. This was necessary to cause the measured resistance values to fall within that range of the conductivity meter's scale that would afford satisfactory readings and interpolations.

d) After each experimental run, the crystallization vessel was caustic-cleaned to remove any trihydrate deposited on the inner walls. Caustic-cleaning consisted of filling the vessel with concentrated NaOH solution (5-8 M), heating this solution to about 80°C, and allowing it to slowly cool. The same cleaning solution was used to clean the vessel after each run.

e) Charges of seed and impurity were made through one of the necks used to hold the electrodes. A funnel type device was used to facilitate the addition.

f) The dried crystalline product from each run was sieved for 20 minutes in a Roto-tap. The resultant size distributions were based on the following screens: NBS #100, #140, #200, and #230. For a description of these screens, refer to Appendix F. Since relatively large flakes and cakes of crystalline trihydrate were formed during the drying

periods (Section III-2g), a NBS #35 screen was used in conjunction with the other screens to exclude these larger particles from the analyses. Thus, the results of the sieve analyses pertain only to that trihydrate capable of passing through the #35 screen. It should be pointed out that most of those relatively large cakes formed during the drying periods were disintegrated during the screening process, so that actually very little material was retained on the #35 screen and discarded.

g) Not all of the crystalline product from a specific run could be recovered, as a portion always remained adhering to the wall of the crystallization vessel. Thus, the sieve analyses represent only the size distributions of the recoverable portions of the crystalline product.

CHAPTER IV

DISCUSSION OF RESULTS

1. General

On the basis of the experimental data a number of aspects of the crystallization step may be analyzed. These include the following factors:

a) Induction period -- "Induction period" is defined as that interval between the time that seed is added to the supersaturated solution and the time that decomposition is first noted. In other words, the induction period is that time period immediately after the seed charge during which the resistance of the solution is constant. In the case of Run #31, which had no seed charge, the induction period is assumed to have begun when the crystallization vessel was immersed in the isothermal reservoir.

b) Initial decomposition rate -- This rate is determined at the end of the induction period, i.e., at the beginning of the decomposition period. For those runs exhibiting no induction periods, the initial decomposition rates are evaluated at time zero (when the seed charge is made). The rates are evaluated as follows: Each run had an initial alumina concentration of 30.6 gpl (16.2 gpl Al is equivalent to 30.6 gpl Al_2O_3). The final alumina concentration was determined analytically.[25] Thus, the total decrease in the alumina concentration is known for each run. Let this decrease be designated $\Delta A_{tot.}$. Let the overall drop in

electrical resistance due to decomposition be designated as $\Delta R_{tot.}$ for a specific run. At the beginning of a run, when decomposition has not occurred to an appreciable degree, it is assumed that a per cent change in resistance approximates the same per cent change in alumina concentration. This assumption is not valid for the entire curve as has been discussed in Section II-2b. Thus, $\Delta R_{initial}/hr$ divided by $\Delta R_{tot.}$ is approximately equal to $\Delta A_{initial}/hr$ divided by $\Delta A_{tot.}$. That is,

$$\frac{\Delta R_{initial}}{hr - \Delta R_{tot.}} \sim \frac{\Delta A_{initial}}{hr - \Delta A_{tot.}}$$

$\Delta R_{initial}/hr$ is merely the slope of the resistance-time curve at the beginning of the decomposition period. Therefore, $\Delta A_{initial}/hr$ is readily evaluated. $\Delta A_{initial}/hr$ times the volume (4 liters) of the decomposing solution gives the initial rate of decomposition in units of grams Al_2O_3/hr. Summarizing, the initial decomposition rate is determined by the equation:

$$I.D.R. = \frac{\Delta R_{initial}}{hr} \times \frac{\Delta A_{tot.}}{\Delta R_{tot.}} \times V$$

where I.D.R. = initial decomposition rate, grams of dissolved Al_2O_3 per hour

$\frac{\Delta R_{initial}}{hr}$ = slope of the resistance-time curve at the beginning of the decomposition period, ohms/hr

$\Delta A_{tot.}$ = overall drop in dissolved alumina, gpl Al_2O_3

$\Delta R_{tot.}$ = overall drop in resistance, ohms

V = volume of system, liters. For all runs, V = 4 liters.

c) "Equilibrium concentrations" -- The alumina concentrations at the terminations of the runs are designated "equilibrium concentrations." It is realized that a condition of equilibrium probably did not exist

for any of the runs, but because the final resistance measurements indicated such small decomposition rates, the designation, "equilibrium concentration," is considered a justifiable approximation.

d) Crystal size distributions -- Size distributions of the crystalline products were obtained as described in Chapter III. Similar information for the initial seed charges may be found in Appendix D.

A discussion of the effects of the investigated impurities on the above aspects of the crystallization step follows immediately. This discussion is sub-divided into five parts, corresponding to the five different major types of experimental runs, namely:

a) Runs with seed charges only (8)

b) Runs with seed and sodium oxalate charges (4)

c) Runs with seed and starch charges (7)

d) Runs with seed and magnesium charges (7)

e) Run without seed or impurity charge (1)

2. Runs with Seed Charges Only

A study of impurity effects can more intelligently be treated if a basis for comparison is available. For this reason a number of runs were made with different seed charges, but with no impurity charges. It was felt that these runs would prove to be valuable standards against which the effects of impurities could be better evaluated. The resistance-time curves for these runs are presented in Figures 8 and 9. Other results pertinent to these runs are found in Table II.

a) Induction periods -- The induction period is a measure of the stability of the given sodium aluminate solution. This stability is related to the tendency for the aluminate ions to decompose to colloidal

Figure 8. Runs with Seed Charges Only

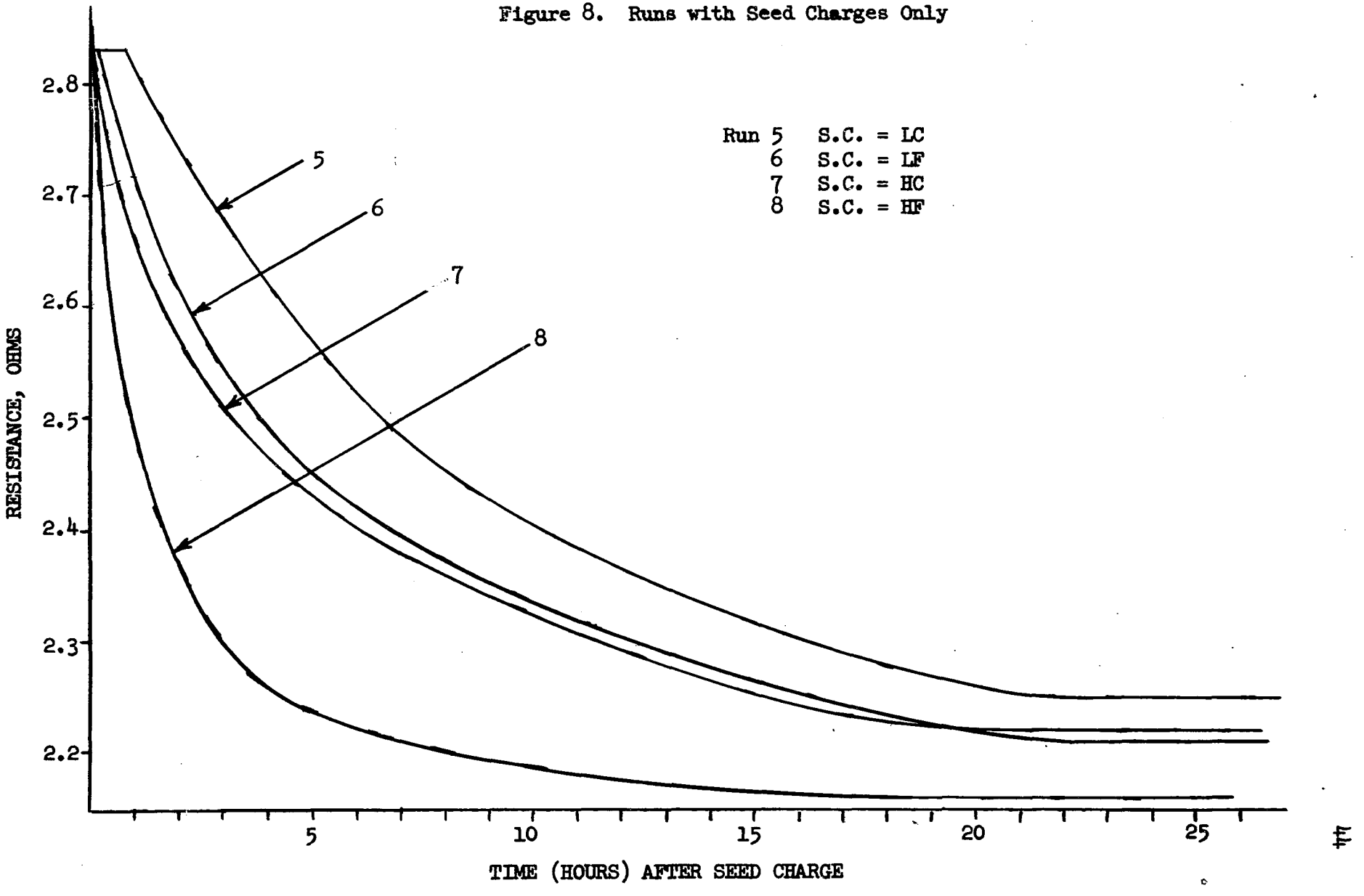

Figure 9. Runs with Seed Charges Only

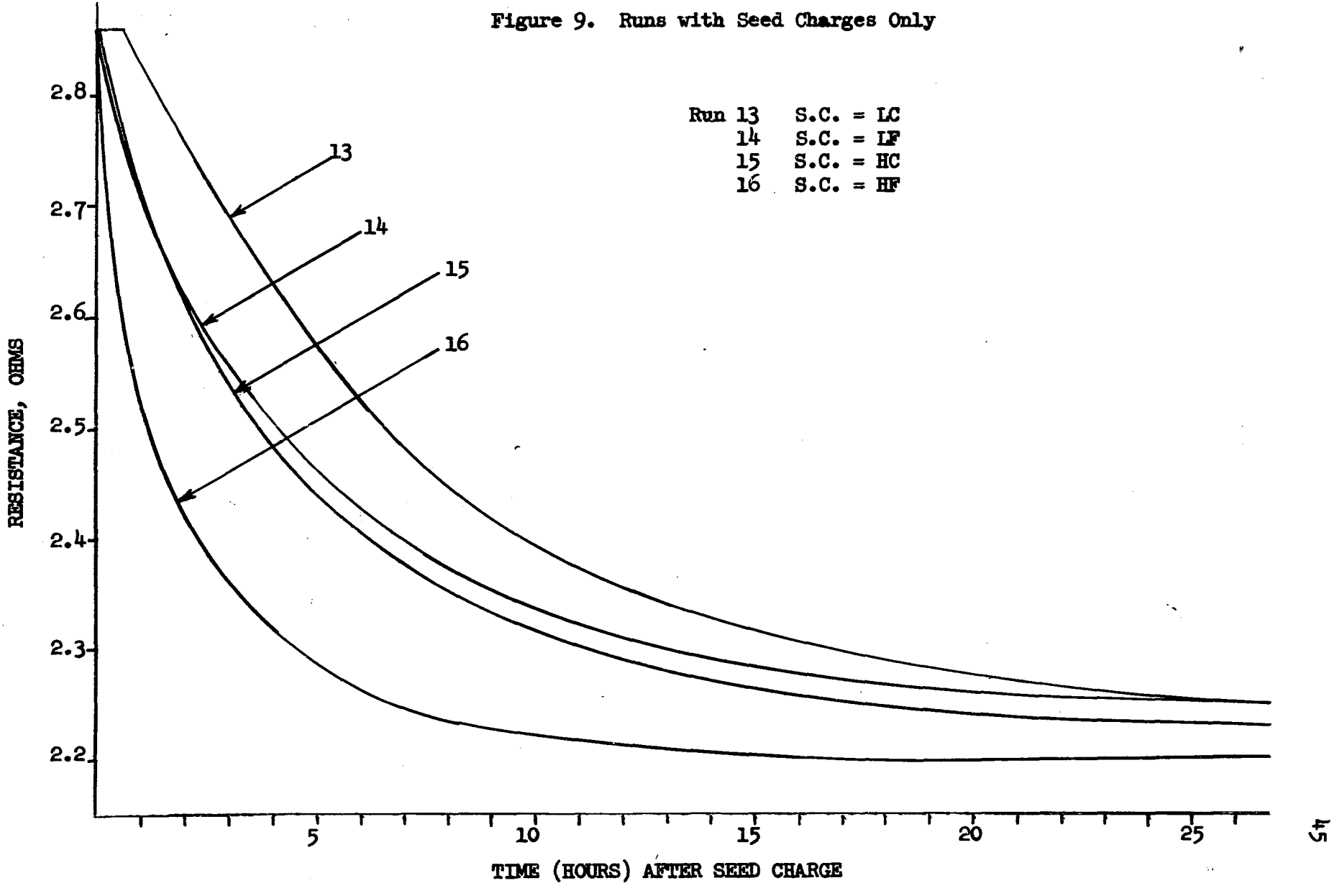

TABLE II

SUMMARY OF DATA FOR RUNS WITH SEED CHARGES ONLY

Run	Seed Charge (S.C.)	Induction Period, min.	Initial Decomposition Rate (I.D.R.), gph Al_2O_3	"Equilibrium Concentration," gpl Al_2O_3
5	LC	45	6.7	17.0
6	LF	8	13.4	17.0
7	HC	3	21.7	16.3
8	HF	0	62.7	15.6
13	LC	38	6.1	18.0
14	LF	0	15.0**	-*
15	HC	3	16.1	17.0
16	HF	0	64.0	15.3

Sieve Analyses, % of Sample

	Run 13	Run 14	Run 15	Run 16
-35 to +100	22.9	1.3	36.9	.2
-100 to +140	19.3	1.4	24.0	.5
-140 to +200	6.8	19.7	19.4	2.7
-200 to +230	.4	19.7	2.2	2.3
-230	50.6	57.9	17.5	94.3

*Sample lost.

**Based on assumed "equilibrium concentration" of 18.0 gpl Al_2O_3.

aluminum hydroxide, which, in turn, depends on the tendency for the conversion from colloidal to crystalline material and deposition of this material on an existing crystal surface. Therefore, all other factors being equal, the greater the total seed surface, the shorter will be the induction period. This relationship is indicated in Figures 8 and 9 and in Table II. The discrepancies between the induction periods of Runs 5-8 and their respective duplicates, Runs 13-16, are not considered significant.

b) Initial decomposition rates -- The decomposition rate for a given sodium aluminate solution depends on the quantity of surface area available for growth, all other factors being equal. Values for initial decomposition rates are presented in Table II. The rates for the two sets of duplicate runs (Runs 5-8 and 13-16) are in satisfactory agreement.

c) "Equilibrium concentrations" -- The data show that the greater the surface area of the seed charge, the lower will be the "equilibrium concentration" of dissolved Al_2O_3.

d) Crystal size distributions -- Table II presents the sieve analyses for Runs 13-16. Similar data for Runs 5-8 were not obtained. Two points are worthy of discussion. (1) Note the difference in the size distributions of Runs 13 and 15, both of which were charged with coarse seed. The product from Run 13 is much finer than that of Run 15. This may be rationalized as follows. Run 13 received a light charge of seed which provided a smaller surface area than did the heavy charge of Run 15. As the sodium aluminate solutions decomposed to yield material available for deposition, the heavy seed charge of Run 15 was inherently more likely to produce less pronounced spires and needle-like growths than

the light charge of Run 13, because its greater area permitted a more uniform growth to occur. During the course of the runs, these spires and needles were knocked off due to agitation, with these new particles serving as more fine seed. Fewer of these fine seed particles were formed in Run 15 than in Run 13. Consequently, the per cent fines in Run 13 is greater than in Run 15, as experimentally shown. (2) Runs 14 and 16 received light and heavy charges of fine seed respectively. Although the preceding explanation should also apply to these runs, it is noted that Run 16 has the finer product. This is probably because the greater number of fines formed by attrition in Run 14 was relatively insignificant when compared to the large amount of fines initially present in the seed charge of Run 16.

3. Runs With Seed and Sodium Oxalate Charges

Figure 10 and Table III present the experimental results of Runs 9-12, i.e., the runs pertinent to the effects of sodium oxalate charges. All of these runs were conducted in an identical manner except for the seed charges, which were varied as indicated.

a) Induction periods -- The induction periods of the oxalate runs (Runs 9-12) appear to be more pronounced than for the runs without any impurity charges (Runs 5-8, 13-16). A suggested explanation is that the presence of the sodium ions resulting from the dissolution of the sodium oxalate charge tended to inhibit and retard the decomposition of sodium aluminate molecules (Equation II-5), the consequent increase in stability of these molecules resulting in correspondingly increased induction periods.

b) Initial decomposition rates -- As seen from Table III, the initial

Figure 10. Runs with Seed and Sodium Oxalate Charges

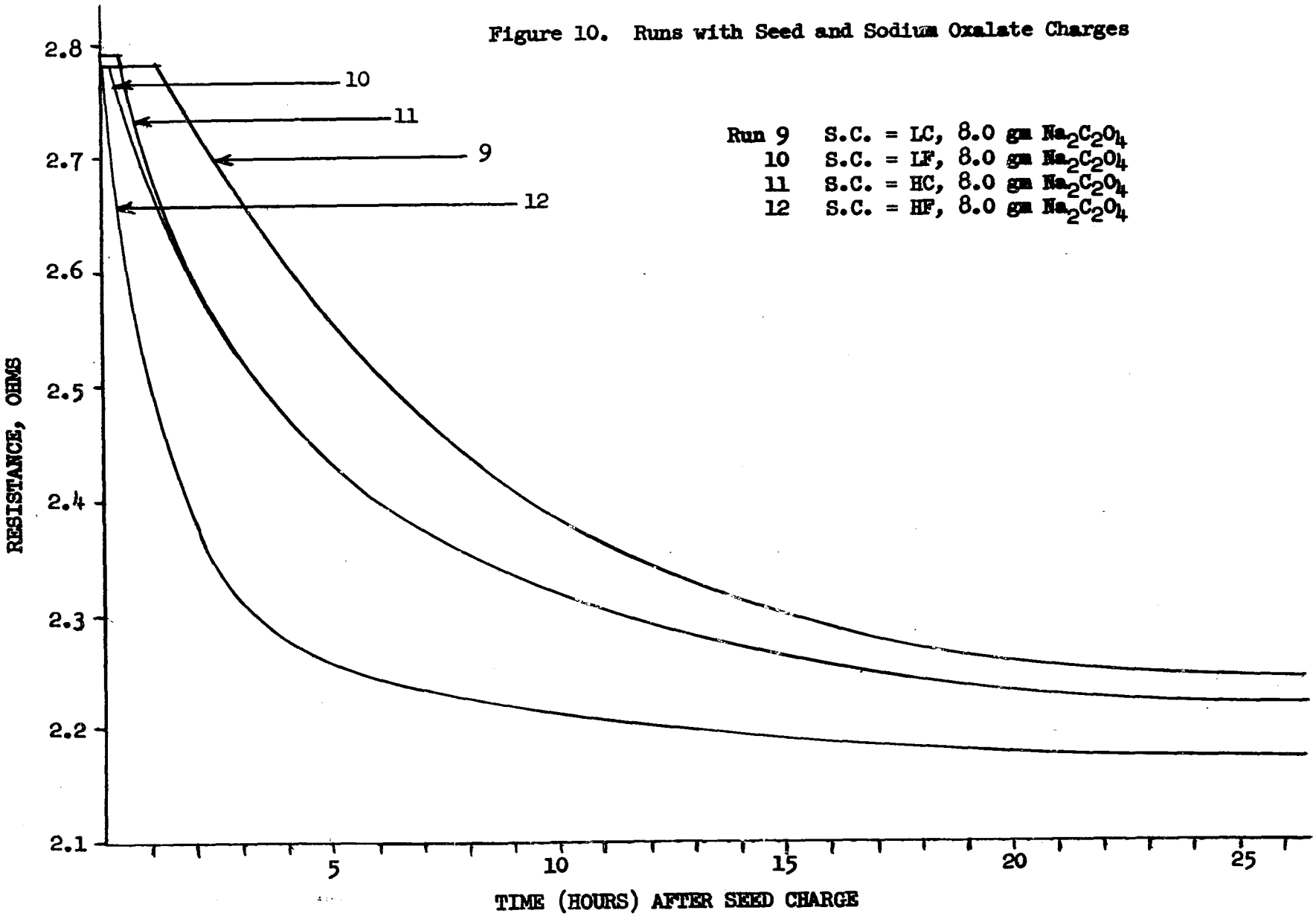

TABLE III

SUMMARY OF DATA FOR RUNS WITH SEED AND SODIUM OXALATE CHARGES

Run	Seed Charge (S.C.)	Oxalate Charge, gm	Induction Period, min.	Initial Decomposition Rate (I.D.R.), gph Al_2O_3	"Equilibrium Concentrations," gpl Al_2O_3
9	LC	8.0	75	6.5	17.7
10	LF	8.0	10	12.4	17.7
11	HC	8.0	20	13.6	17.3
12	HF	8.0	0	45.0	15.0

Sieve Analyses, % of Sample

	Run 9	Run 10	Run 11	Run 12
-35 to +100	.85	.3	35.7	.3
-100 to +140	1.17	.9	29.0	.6
-140 to +200	1.70	14.1	17.3	2.8
-200 to +230	.28	22.4	2.3	2.0
-230	96.00	62.3	15.7	94.3

decomposition rates for the oxalate runs show the expected variation with type of seed charge. However, the I.D.R. values for the oxalate runs are appreciably lower than the corresponding values for those runs without impurities. This may be attributed to the decrease in the decomposition tendency due to the presence of the additional sodium ions. Since rate equals driving force divided by resistance, a decrease in the driving force (decomposition tendency) produces a proportional decrease in rate.

c) "Equilibrium concentrations" -- Comparisons of these values for the oxalate runs and the "pure" runs (Runs 5-8, 13-16) indicate little difference. Apparently, sodium oxalate serves to slow the decomposition process without appreciably affecting the end results.

d) Crystal size distributions -- The oxalate appears to have little effect upon the final size distribution of the product crystals. This conclusion is made on the basis of the sieve analyses found in Tables II and III. Excellent agreement is noted between Runs 14-16 of the "pure" runs and Runs 10-12 of the oxalate runs. The discrepancy between the size distributions of Run 13 ("pure") and 9 (oxalate) is not accounted for.

Summarizing the experimental results for Runs 9-12, it is concluded that, for the given solutions and charges, the only significant effect due to the presence of sodium oxalate is a small decrease in the decomposition tendency. This may result in a slightly longer induction period and a slower crystallization rate. This conclusion corroborates Pearson's opinion that industrial concentrations of sodium oxalate have a negligible effect on the crystallization step.

4. Runs With Seed and Starch Charges

The experimental results of the starch runs (Runs 17-20, 28-30) are found in Figures 11 and 12 and Table IV.

a) Induction periods -- Runs 17 and 18 were terminated without decomposition after roughly 20 and 10 hours, respectively. All the other runs decomposed after the various induction periods listed in Table IV. It is apparent that starch very effectively prolongs the induction period. The following explanation may account for this phenomenon. Dean[2] emphasizes that the metal hydroxides exhibit strong tendencies to adsorb hydroxyl and hydrogen ions. The glucose rings of starch contain a number of these groups (H and OH), which could cause the starch to be adsorbed by the metallic hydroxide. In the case of the alumina trihydrate seed particles, such an adsorption of starch would result in a decrease in the effective surface area available for crystal growth. A sufficiently high starch concentration could possibly permanently inhibit crystal growth, e.g., Runs 17 and 18. The coating property of soluble starch is also attested to by Lewis, Squires and Broughton.[15] They maintain that soluble starch is an excellent protective colloid, the protective action stemming from the adsorption of the starch to form an envelope or skin of hydrophilic material about the adsorbing particles. Such a mechanism could effectively repress the adsorption and surface orientation of any newly formed trihydrate material by the "poisoned" seed, thereby inhibiting crystal growth significantly and producing lengthy, if not interminable, induction periods.

Another mechanism that might account for the effects of starch is suggested by Moeller[18] in his discussion of complex ions and coordi-

Figure 11. Runs with Seed and Starch Charges

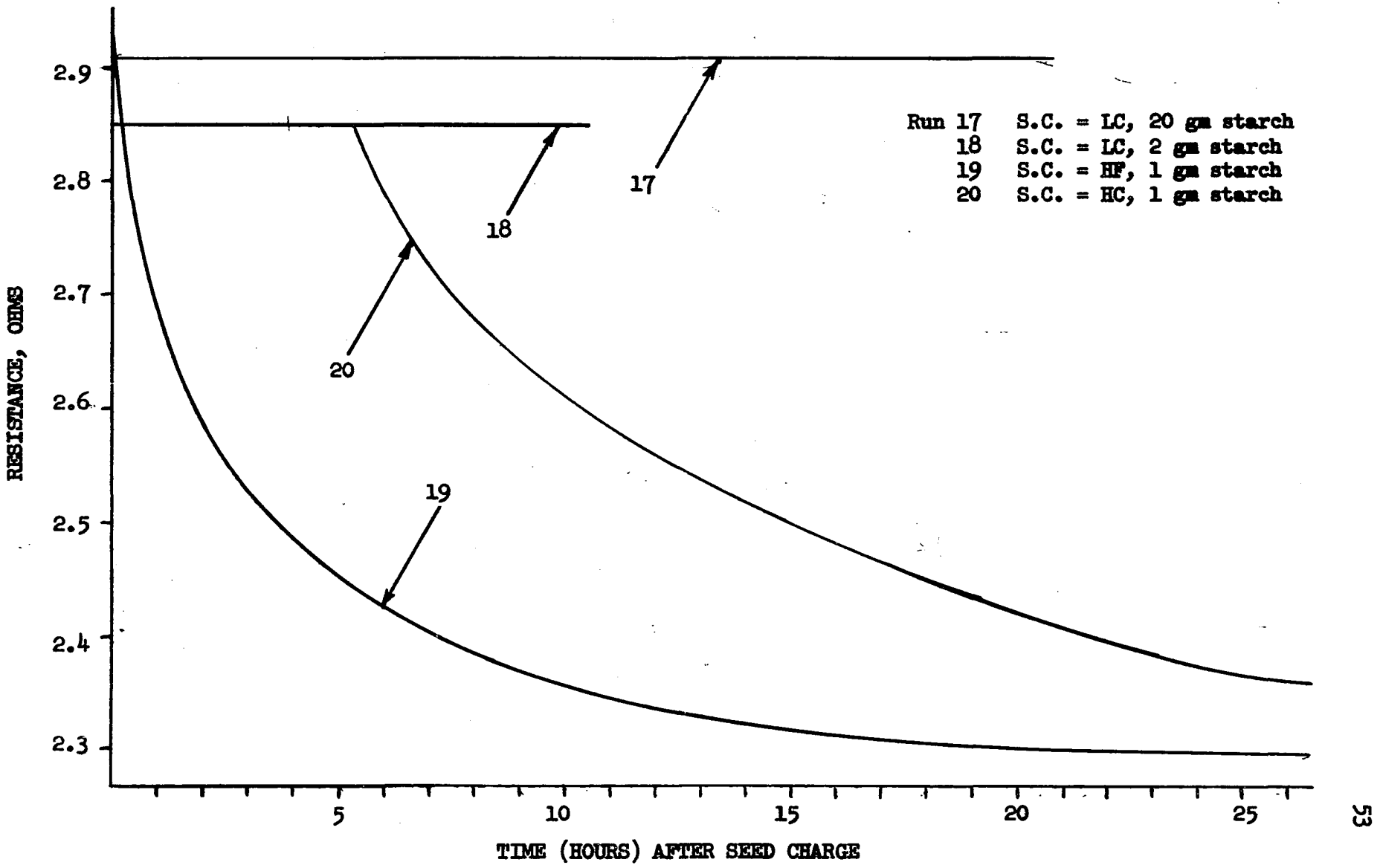

Figure 12. Runs with Seed and Starch Charges

Run 28 S.C. = LF, .25 gm starch
29 S.C. = LF, 1.0 gm starch
30 S.C. = LF, .1 gm starch

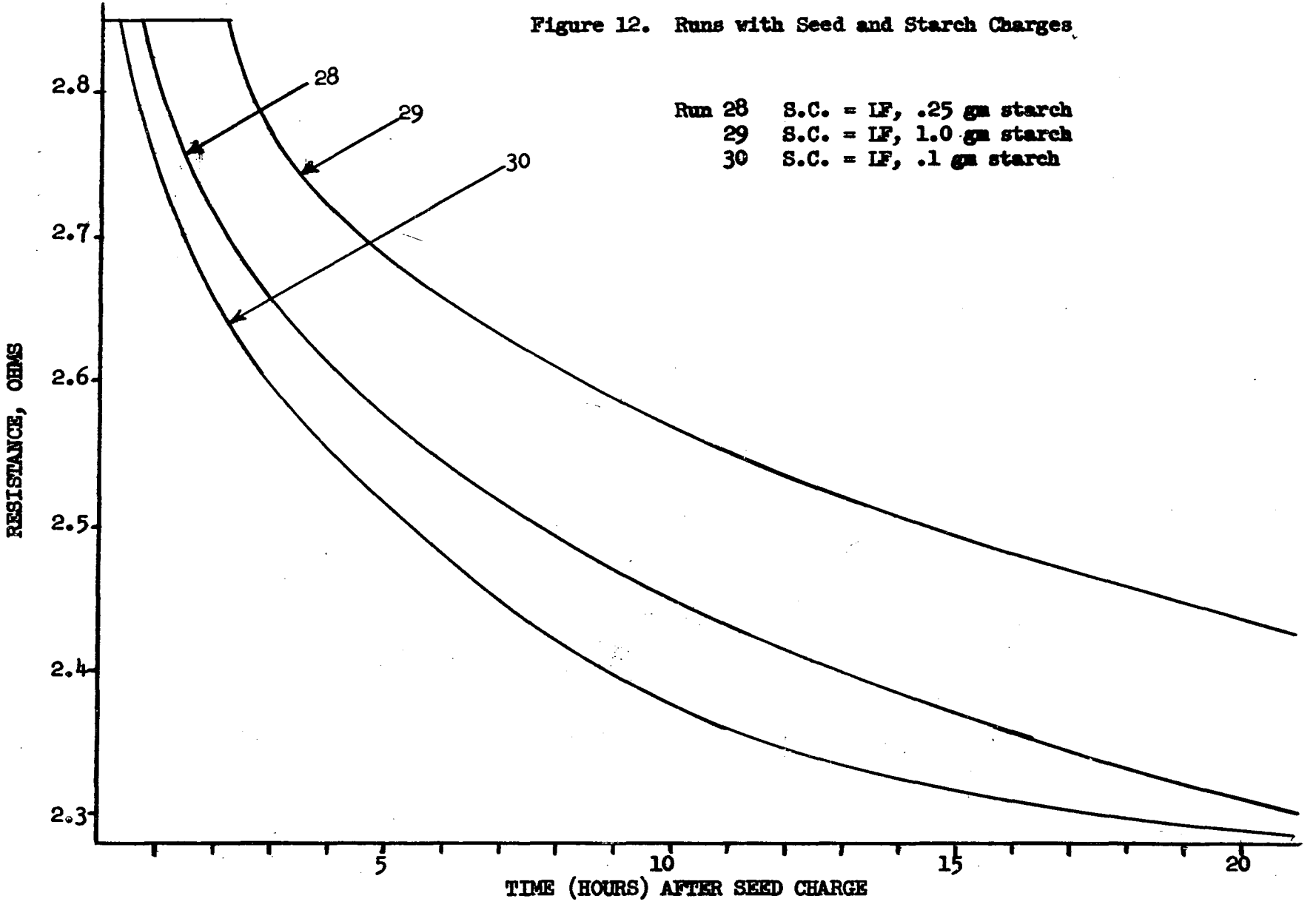

TABLE IV

SUMMARY OF DATA FOR RUNS WITH SEED AND STARCH CHARGES

Run	Seed Charge (S.C.)	Starch Charge, gm	Induction Period, min.	Initial Decomposition Rate (I.D.R.), gph Al_2O_3	"Equilibrium Concentration," gpl Al_2O_3
17	LC	20	1230+	-	-
18	LC	2	615+	-	-
19	HF	1	0	25.6	18.0
20	HC	1	320	9.7	19.7
28	LF	25	45	10.5	20.7
29	LF	1	135	11.0	21.1
30	LF	0.1	23	14.3	17.7

Sieve Analyses, % of Sample

	Run					
	17	19	20	28	29	30
-35 to +100	29.5	.4	46.7	.6	2.2	4.7
-100 to +140	30.9	.5	33.5	2.5	6.1	4.4
-140 to +200	21.9	3.5	18.5	39.8	53.0	26.7
-200 to +230	4.8	3.1	.8	26.0	22.4	19.3
-230	12.9	92.5	.5	32.1	16.3	44.9

nation compounds. It is possible that the Al^{+3} ion is complexed by the OH^- groups of the starch to form soluble complex anions. The subsequent formation of colloidal alumina trihydroxide would be inhibited by the soluble nature of the complex, thus yielding prolonged induction periods. However, microphotographs of crystal products from the starch runs are more readily interpreted on the basis of the "surface-shielding" mechanism than this latter mechanism. These photographs are discussed in Section IV-7.

b) Initial decomposition rates -- Starch serves to reduce the initial decomposition rates very appreciably. For example, compare Runs 19 and 20 with their "pure" counterparts, Runs 8, 16 and 7, 15. A starch charge of only 1 gm was sufficient to reduce the I.D.R.'s of the "pure" runs by roughly 50%. This retardation of the decomposition process may be attributed to the decrease of effective seed surface due to starch adsorption.

c) "Equilibrium concentrations" -- These values for the starch runs are considerably higher than the corresponding values for the "pure" runs of Table II. This may be due to the virtual elimination of effective crystal growth area by the surface adsorption of starch. Another possible explanation is that the aluminate ions themselves are stabilized by starch "envelopes" and, consequently, have a lessened tendency to decompose.

d) Crystal size distributions -- Note the sieve analyses of Runs 28-30, all of which received light, fine (LF) seed charges. The tendency toward a fine product increases from Run 29 to Run 30. However, the starch charges decrease in the same order. This is evidence of the agglomerating nature of soluble starch. This agglomeration of crystals

by action of the starch also helps to account for the decrease in effective surface area previously mentioned. The size distribution of the crystals from Run 17 is essentially the same as the size distribution of its coarse seed charge. For some reason (no decomposition was noted for this run), the original seed charge exhibited little tendency to agglomerate, even in the presence of a very heavy starch charge. The size distributions of Runs 19 and 20 are not unusual and will receive no discussion.

A summary of the results of the starch runs should include the following points: first, unlike sodium oxalate, starch appears to affect all aspects of the crystallization step; second, the effects of starch may be due to its adsorption on the surfaces of crystal particles; third, a sufficiently large starch charge may permanently inhibit crystal growth; and finally, no optimum starch charge---as was mentioned by Sato[23]---was found for the solutions and charges investigated.

5. Runs With Seed and Magnesium Charges

The results pertinent to these runs (Runs 21-27) are found in Figures 13 and 14 and Table V. All charged magnesium was in the form of basic magnesium carbonate, $4MgCO_3 \cdot Mg(OH)_2 \cdot 5H_2O$. For lack of complete solubility data for this compound, the following assumptions were made: (1) Magnesium charges of 0.25 and 1.0 gm were completely soluble, and (2) The 3-gm magnesium charge probably was sufficient to saturate the decomposing solution with some of the solid charge remaining in suspension.

In filtering the product crystals from the magnesium runs, a "milky" appearance was noted in the supernatant liquid that was not apparent in

Figure 13. Runs with Seed and Magnesium Charges

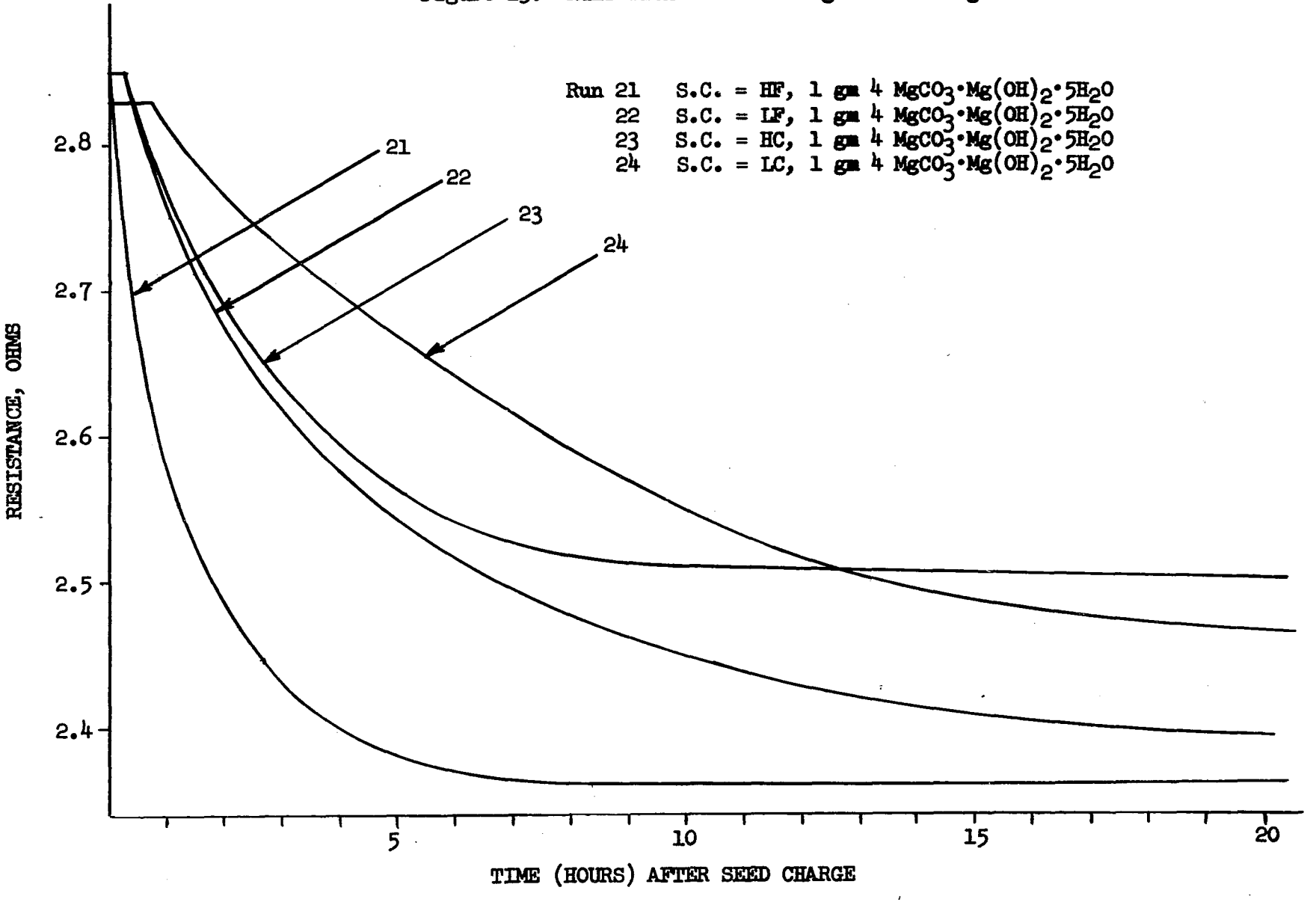

Figure 14. Runs with Seed and Magnesium Charges

Run 25 S.C. = LF, 3 gm $4MgCO_3 \cdot Mg(OH)_2 \cdot 5H_2O$
26 S.C. = LF, 1 gm $4MgCO_3 \cdot Mg(OH)_2 \cdot 5H_2O$
27 S.C. = LF, .25 gm $4MgCO_3 \cdot Mg(OH)_2 \cdot 5H_2O$

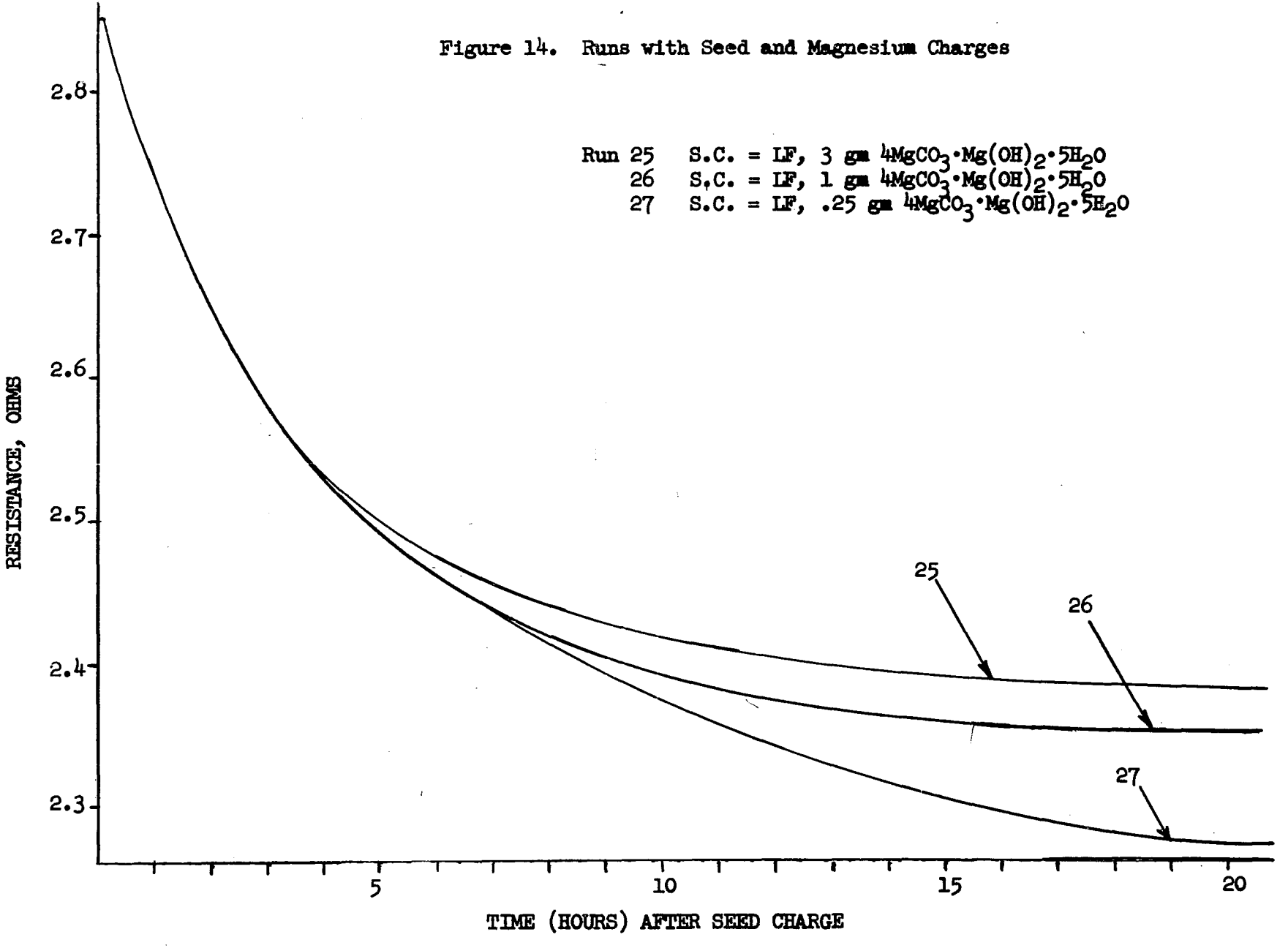

TABLE V

SUMMARY OF DATA FOR RUNS WITH SEED AND MAGNESIUM CHARGES

Run	Seed Charge (S.C.)	Magnesium Charge, gm $4MgCO_3 \cdot Mg(OH)_2 \cdot 5H_2O$	Induction Period, min.	Initial Decomposition Rate (I.D.R.), gph Al_2O_3	"Equilibrium Concentration," gpl Al_2O_3
21	HF	1	0	35.6	19.7
22	LF	1	15	12.8	20.7
23	HC	1	15	11.1	24.1
24	LC	1	45	4.7	23.8
25	LF	3	5	11.9	21.4
26	LF	1	5	11.5	21.1
27	LF	.25	5	11.7	19.4

Sieve Analyses, % of Sample

	Run						
	21	22	23	24	25	26	27
-35 to +100	.5	1.1	38.4	40.3	8.4	6.6	5.5
-100 to +140	2.0	2.1	32.3	34.3	7.0	7.1	5.7
-140 to +200	7.5	14.1	23.0	8.7	15.3	19.9	23.6
-200 to +230	3.8	10.0	2.7	.6	9.0	11.4	12.8
-230	86.2	72.7	3.6	16.1	60.3	55.0	52.4

the other runs (Runs 5-20, 28-30). Also, the filter cake of product crystals from each magnesium run offered considerably more resistance to filtration than was noted for any of the nonmagnesium runs. One possible explanation for these characteristics is that the transformation from the colloidal $Al(OH)_3 \cdot (H_2O)_3$ to the crystalline $Al_2O_3 \cdot 3H_2O$, i.e.,

$$\underset{\text{colloidal}}{2Al(OH)_3 \cdot (H_2O)_3} + 2NaOH \longrightarrow \underset{\text{crystalline}}{Al_2O_3 \cdot 3H_2O} + 2NaOH + 6H_2O \qquad \text{(II-6)}$$

was somehow inhibited, causing an appreciable amount of the decomposition product to remain in the colloidal stage. Kolthoff and Sandell[12] stress that such precipitates are difficult to filter and purify by a washing process, having a marked tendency to clog the filter medium. The experimentally observed "milkiness" could also be attributed to the presence of such colloidal particles.

a) Induction periods -- For the magnesium charges investigated, no significant effects on the induction periods of any of the runs are noted. For Runs 25-27, in which the magnesium charges vary by 1200%, the absence of effects upon the induction periods is particularly obvious. In general, the induction periods of all the magnesium runs are essentially identical with the induction periods of the "pure" run counterparts, as found in Table II.

b) Initial decomposition rates -- The I.D.R. values for the magnesium runs are appreciably less than those of the corresponding "pure" runs. Dean[2] indicates that when aluminum hydroxide, $Al(OH)_3 \cdot (H_2O)_3$, is precipitated from a basic solution, hydroxyl ions will be adsorbed and will carry down cations, such as magnesium. The tendency for

adsorption of magnesium is much stronger than that for sodium (which, of course, is also present) because of the principle involved in the Paneth-Fajans rule.[2] This rule states that those ions will be adsorbed which form a relatively insoluble salt with the ions of the opposite charge. As $Mg(OH)_2$ is very insoluble relative to NaOH, the adsorption of magnesium ions is favored. The resultant electrical potentials of these adsorbed magnesium ions could be sufficient to cause the individual colloidal hydroxide particles to repel one another, thus slowing, or even preventing, the conversion of these colloidal particles to the crystalline trihydrate. This explanation accounts for the previously mentioned "milkiness" in the supernatant liquids, the poor filterability of the product crystals, and the reduction in I.D.R. values. The I.D.R. values of Runs 25-27 are remarkably constant in spite of the 1200% variation in magnesium charges. One possible explanation is that the smallest charge (0.25 gm for Run 27) is sufficiently large to provide the maximum number of magnesium ions capable of being adsorbed under the initial conditions.

The mechanism suggested in the preceding paragraph appears to contradict the previously-mentioned conclusions about induction periods. It seems logical that adsorbed magnesium ions, by inhibiting the conversion from colloidal to crystalline form, would thereby tend to reduce the decomposition potential of the aluminate ions, resulting in significantly longer induction periods than were actually observed. This dilemma has not been satisfactorily resolved. An approach to an acceptable explanation runs as follows: At the beginning of a run, virtually no colloidal alumina hydroxide is present, so little or no magnesium has

been adsorbed. Consequently, the initial tendency of the aluminate ions to decompose is roughly the same in the magnesium runs as in the corresponding "pure" runs, and approximately equal induction periods will result. However, once decomposition is initiated and colloidal material is present, this colloidal material will preferentially adsorb magnesium ions, resulting in the subsequent slower decomposition rates that are reflected by the I.D.R. values of Table V.

c) "Equilibrium concentrations" -- The trend is for an increase in the "equilibrium concentration" of dissolved alumina with an increase in magnesium charge, the seed charge remaining constant. Comparing Run 27 with its corresponding "pure" run, Run 6, the effect of even a small concentration of magnesium (e.g., a magnesium charge of 0.25 gm) is apparent.

d) Crystal size distributions -- Examination of the results listed in Table V and comparison of these results with the sieve analyses of Table II reveal nothing particularly striking or unique about the magnesium runs. Apparently, magnesium has little, if any, effect on the final product size distributions.

Summarizing the results from the magnesium runs, it is concluded that the addition of magnesium as $4MgCO_3 \cdot Mg(OH)_2 \cdot 5H_2O$ tends to retard the decomposition rates and increase the final dissolved alumina concentration. Effects of this impurity on induction periods and product sizes are not significant.

6. Run Without Seed or Impurity Charge

One run was made using the standard aluminate solution without either seed or impurity charges. This run was conducted isothermally

at 30.8°C. As in the previous runs, the agitator was set to rotate at 1500 rpm. Table VI presents the results of this run.

a) Induction period -- The induction period for this run, approximately 70 hours, is a good example of the stability of supersaturated sodium aluminate solutions. It is expected that, had this run been conducted at 70°C as were all the other runs, the induction period would have been even longer than the observed value.

b) Initial decomposition rate -- A plot of resistance-vs-time would show a curve asymptotic to a horizontal line; i.e., the slope of such a curve would be essentially zero at the start of decomposition. Such a plot is not presented herein.

c) "Equilibrium concentrations" -- This value, 14.5 gpl Al_2O_3, is much lower than the corresponding values for any of the preceding runs. This may be attributed to several things: first, the long running time after initial decomposition (the entire run lasted 10 1/2 days compared to about 26 hours for the other runs); second, the absence of charged impurities which could serve as poisons; and third, the lower temperature for Run 31---30.8°C in contrast to 70.0°C for the others.

d) Crystal size distribution -- The sieve analysis of Table VI shows a rather uniform distribution over the entire range of screens. Comparison with the other sieve analyses shows that the product sizes from Run 31 were clearly more uniformly distributed than the others. This is probably due to the absence of an introduced bias, such as a seed charge, which was present in Runs 5-30.

TABLE VI

SUMMARY OF DATA FOR RUN WITHOUT SEED OR IMPURITY CHARGE

Run	Induction Period, hr	Initial Decomposition Rate (I.D.R.), gph Al_2O_3	"Equilibrium Concentration," gpl Al_2O_3
31	Approx. 70	Approx. 0	14.5

Sieve Analysis, % of Sample

	Run 31
-35 to +100	12.2
-100 to +140	7.3
-140 to +200	34.4
-200 to +230	22.6
-230	23.5

7. Microphotographs of Crystals

Samples of all the product crystals from the various experimental runs were examined under the microscope in an effort to observe and record distinguishing features that could be attributed to the conditions under which the runs were conducted. Seed samples were also examined. Many of the samples were quite similar; others were very unique. Table VII presents a summary of the findings of this visual inspection.

Some representative samples were selected to be microphotographed. The resulting microphotographs are presented as Figures 15-23. Only those crystals that could pass a NBS #230 screen were photographed. This was done to enable all of the crystals in each photo to be reasonably in focus. However, even with this precaution, many objects appear blurred and almost indistinguishable.

Figure 15 is a microphotograph of crystals from Run 16, a "pure" run with a HF seed charge. The crystals are agglomerated into clusters with only a few single crystals evident. Crystals from other "pure" runs, Runs 13-15, are quite similar in appearance to those of Run 16, except for the higher number of single crystals for the former runs. On the basis of this photograph and the observations noted in Table VII, the mechanism of "fines" formation by attrition described in Section IV-2d seems to be reasonable.

Crystals from oxalate run, Run 10, are pictured in Figure 16. This run received a LF seed charge. Notice the decided difference in mean crystal sizes of Figures 15 and 16. This difference may be attributed to the different seed charges. The crystals pictured in Figure 16 are typical of all the oxalate runs, deviations lying only in the relative

numbers of clusters and single crystals.

Figure 17 presents a photograph of crystals from Run 17, which received a LC seed charge and a 20-gram starch charge. This run failed to exhibit decomposition after an induction period of roughly 20 hours. Lack of crystal growth is evident by the absence of single crystals ("fines") or of aciculated clusters. The pictured crystals seem to be the original seed particles that have been enveloped with a layer of starch. This is quite probable in light of the small seed charge and heavy starch charge.

Figures 18 and 19 are photographs of crystals from Runs 29 and 30. Both runs received LF seed charges, but Run 29 received a 1-gram starch charge, Run 30 a 0.1-gram starch charge. The most obvious difference is in the degree of aciculation. This difference is even more apparent from a study of Figures 20 and 21, which are microphotographs of single crystals from Runs 29 and 30 at a greater magnification. Run 29 (Figures 18 and 20) yielded crystals with more extreme aciculae than did Run 30. A possible explanation is that, due to the heavier starch charge of Run 29, certain portions of each seed crystal were effectively shielded, causing all growth to occur over the remaining unshielded seed area. The starch charge for Run 30 was much smaller than for Run 29, so that less seed surface was shielded in Run 30, yielding a more uniform growth and less pronounced aciculae.

Single crystals obtained by breaking up a number of clusters from Run 29 are pictured in Figure 22. These are typical of single crystals found in the products of all the runs, as well as in the seed crystals.

Figure 23 presents a photograph of the fine seed used in all the LF

and HF runs. Figure 24 is a photograph of the crystals that spontaneously nucleated in Run 31. Notice the extreme smallness of the Run 31 crystals relative to the fine seed. This is particularly striking when the long operating time (10 1/2 days) and low "equilibrium concentration" (14.5 gpl Al_2O_3) of Run 31 are considered. The fineness of the product crystals must be attributed to the great initial area available for growth. This initial area resulted from the spontaneous nucleation.

TABLE VII

RESULTS OF MICROSCOPIC INSPECTION OF CRYSTALS*

Run No.	Type Run	Comments
9	LC, 8.0 gm $Na_2C_2O_4$	Many acicular clusters; also, numerous single crystals
10	LF, 8.0 gm $Na_2C_2O_4$	Relatively few single crystals; mostly clusters with pronounced aciculae
11	HC, 8.0 gm $Na_2C_2O_4$	Some single crystals; many acicular clusters
12	HF, 8.0 gm $Na_2C_2O_4$	A few single crystals; mostly clusters
13	LC	Considerable number of both single crystals and clusters
14	LF	Mixture of clusters and single crystals; clusters predominate
15	HC	Mixture of clusters and single crystals; clusters predominate
16	HF	Mostly well-aciculated clusters; very few single crystals
17	LC, 20 gm starch	Uniform, large crystals with complete lack of aciculae
18	LC, 2 gm starch	Uniform, large crystals with only a few having pronounced aciculae
19	HF, 1 gm starch	Small clusters, well pronounced aciculae; a few single crystals
20	HC, 1 gm starch	Small clusters; more single crystals than in Run 19
21	HF, 1 gm basic $MgCO_3$	Clusters with modified aciculae
22	LF, 1 gm basic $MgCO_3$	Uniformly sized clusters; not very acicular

TABLE VII (Continued)

Run No.	Type Run	Comments
23	HC, 1 gm basic $MgCO_3$	Wide size distribution; many single crystals; many clusters
24	LC, 1 gm basic $MgCO_3$	Small clusters, not very acicular; also, some single crystals
25	LF, 3 gm basic $MgCO_3$	Uniform clusters; not very acicular
26	LF, 1 gm basic $MgCO_3$	Uniform clusters; not very acicular
27	LF, .25 gm basic $MgCO_3$	Uniform clusters; not very acicular
28	LF, .25 gm starch	Uniformly sized clusters; well aciculated.
29	LF, 1 gm starch	Some single crystals; mostly well-aciculated clusters
30	LF, 0.1 gm starch	Clusters with very pronounced aciculae; few single crystals
31	Spontaneous precipitation	Extremely small crystals; no clusters
	Fine seed	A few clusters; mostly very small single crystals
	Coarse seed	Mixture of acicular clusters and single crystals

*The microscopic inspection was performed with a magnification of 150. To facilitate the procedure, only the fraction from each crystal batch capable of passing a NBS #230 screen was examined.

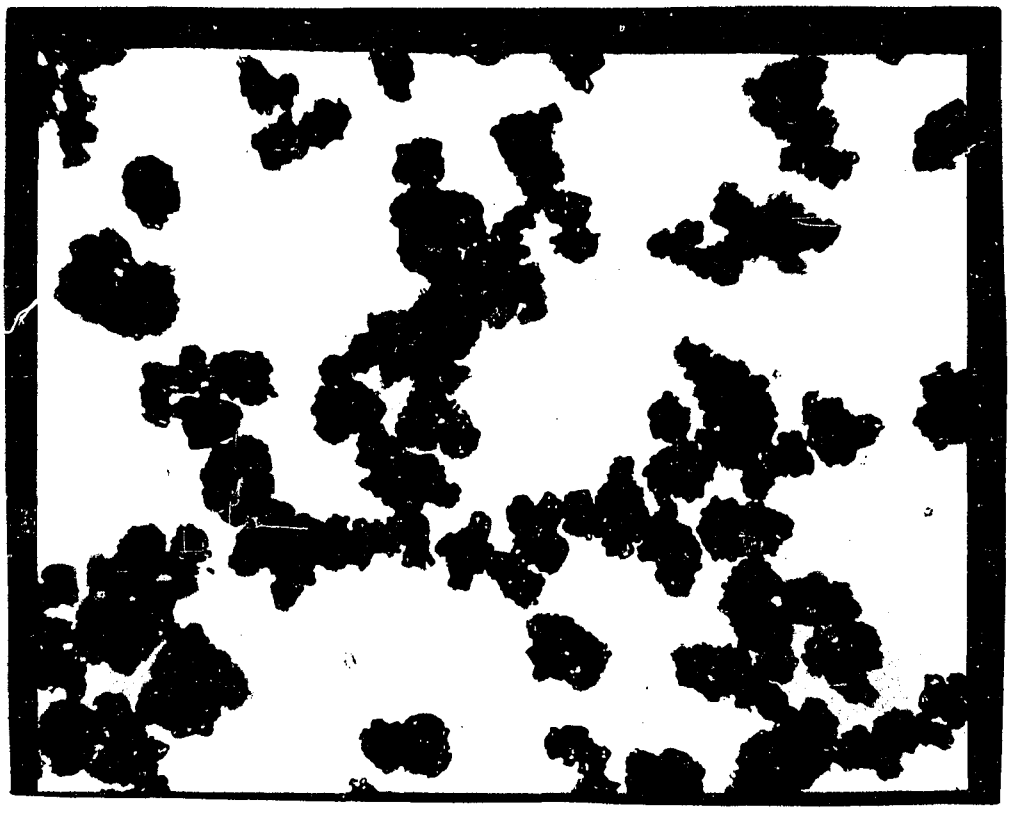

Figure 15. Microphotograph of Crystals from Run 16 (200X)

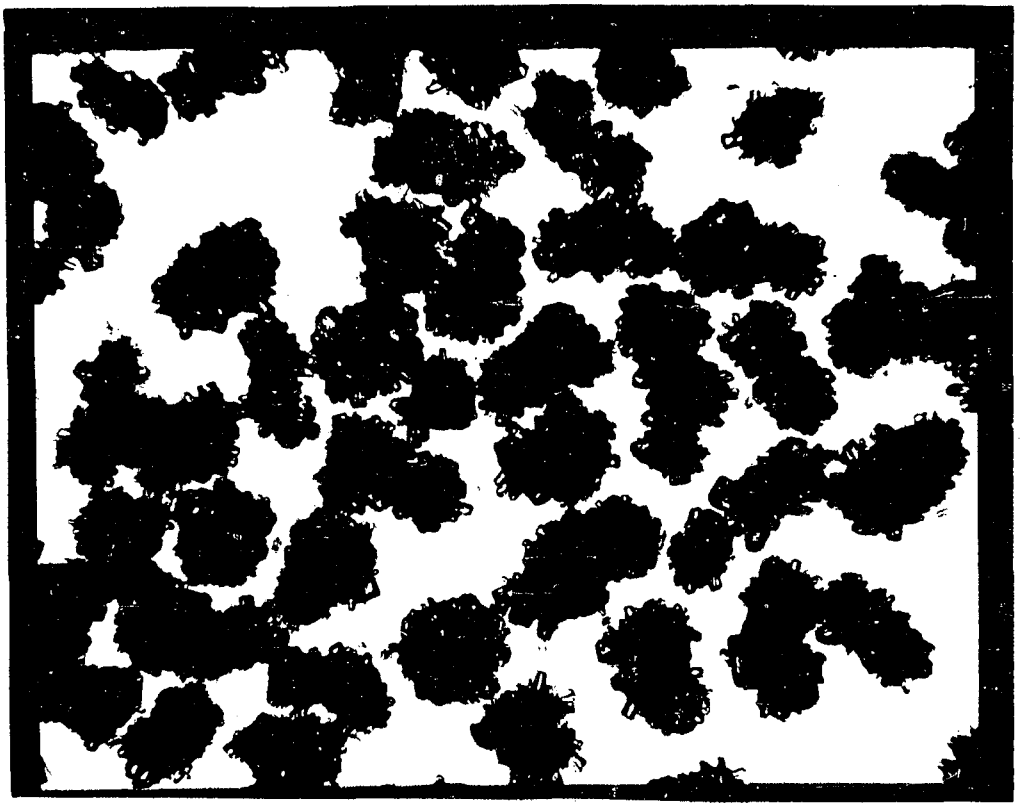

Figure 16. Microphotograph of Crystals from Run 10 (200X)

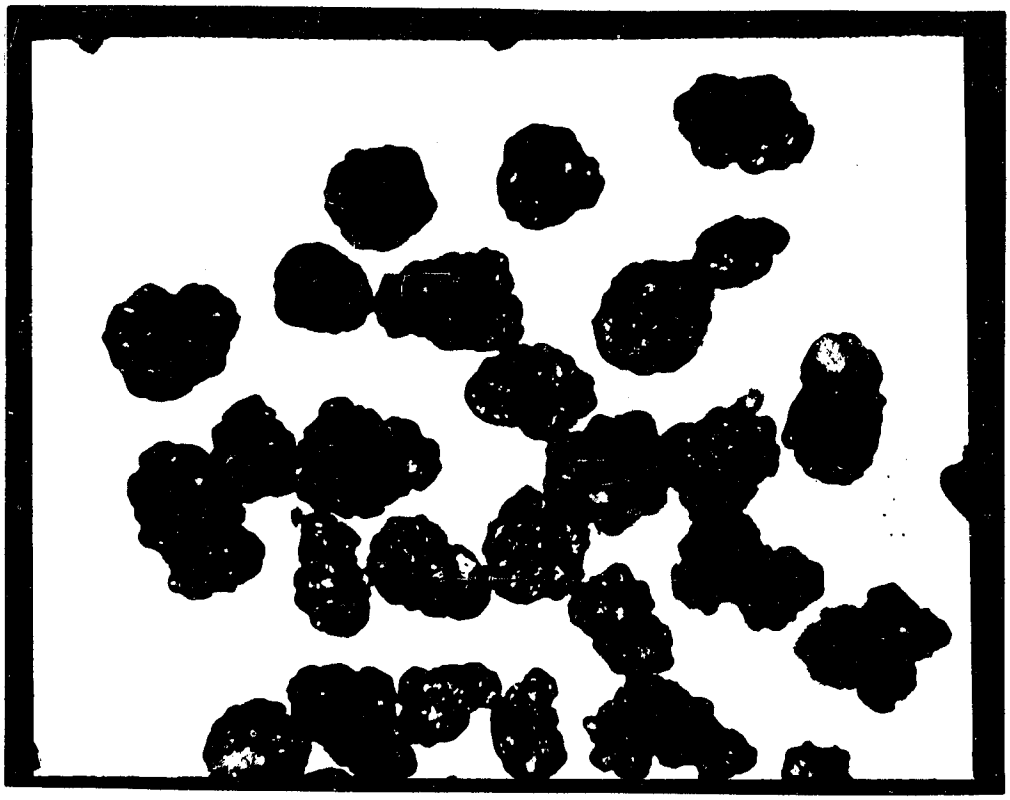

Figure 17. Microphotograph of Crystals from Run 17 (200X)

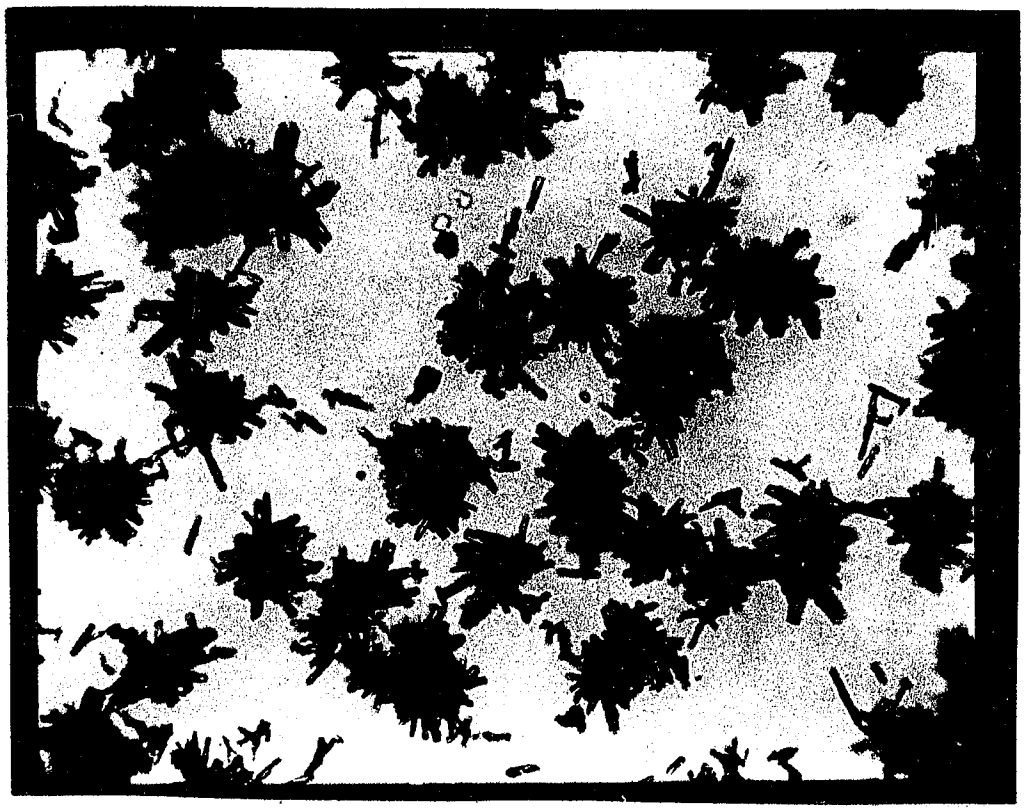

Figure 18. Microphotograph of Crystals from Run 29 (200X)

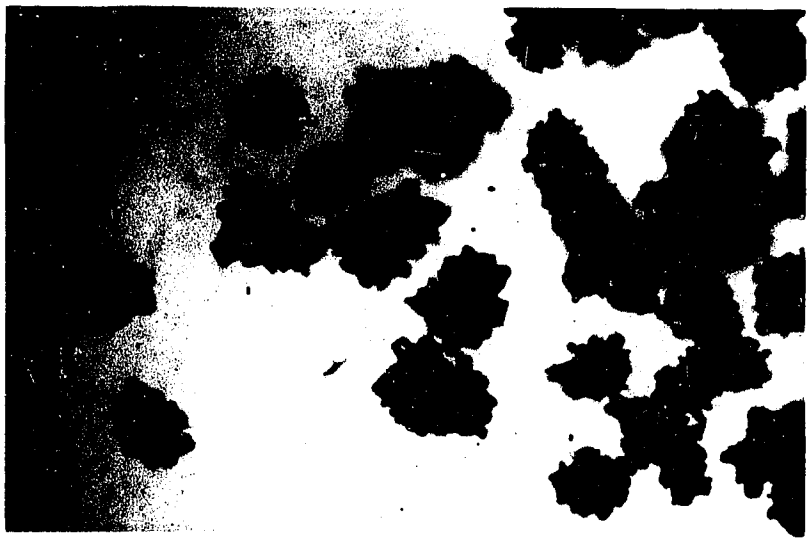

Figure 19. Microphotograph of Crystals from Run 30 (120X)

Figure 20. Microphotograph of a Cluster from Run 29 (540X)

Figure 21. Microphotograph of a Cluster from Run 30 (540X)

Figure 22. Microphotograph of Crystals from Run 29 (400X)

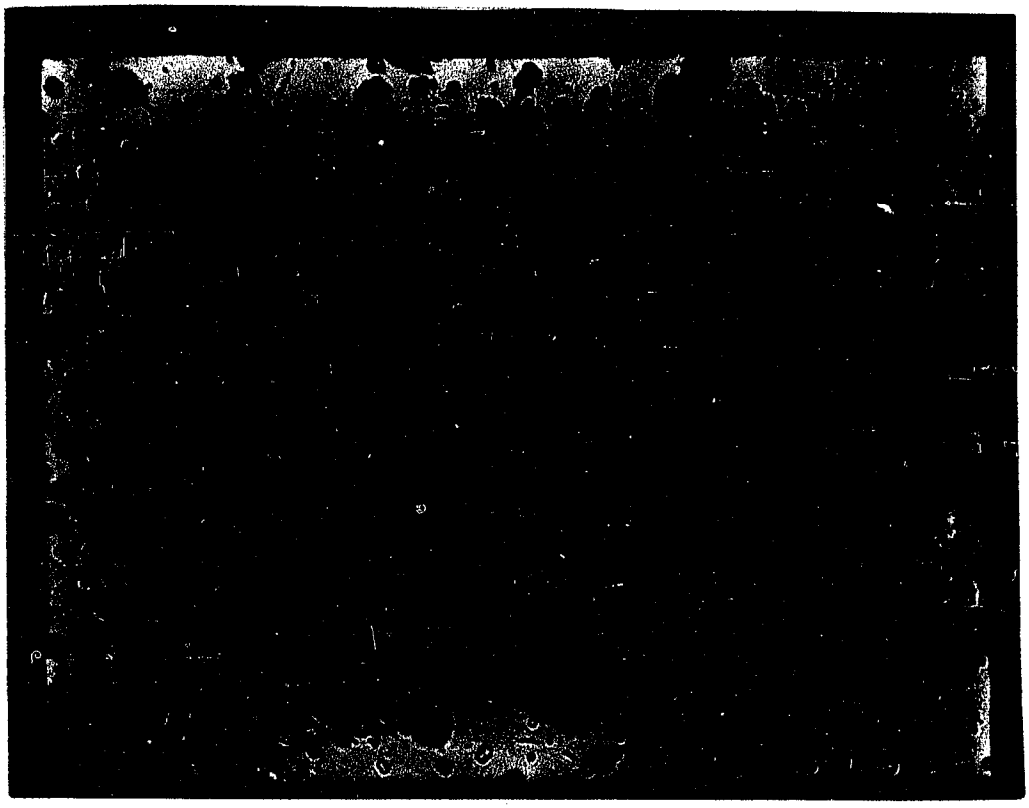

Figure 23. Microphotograph of Fine Seed (400X)

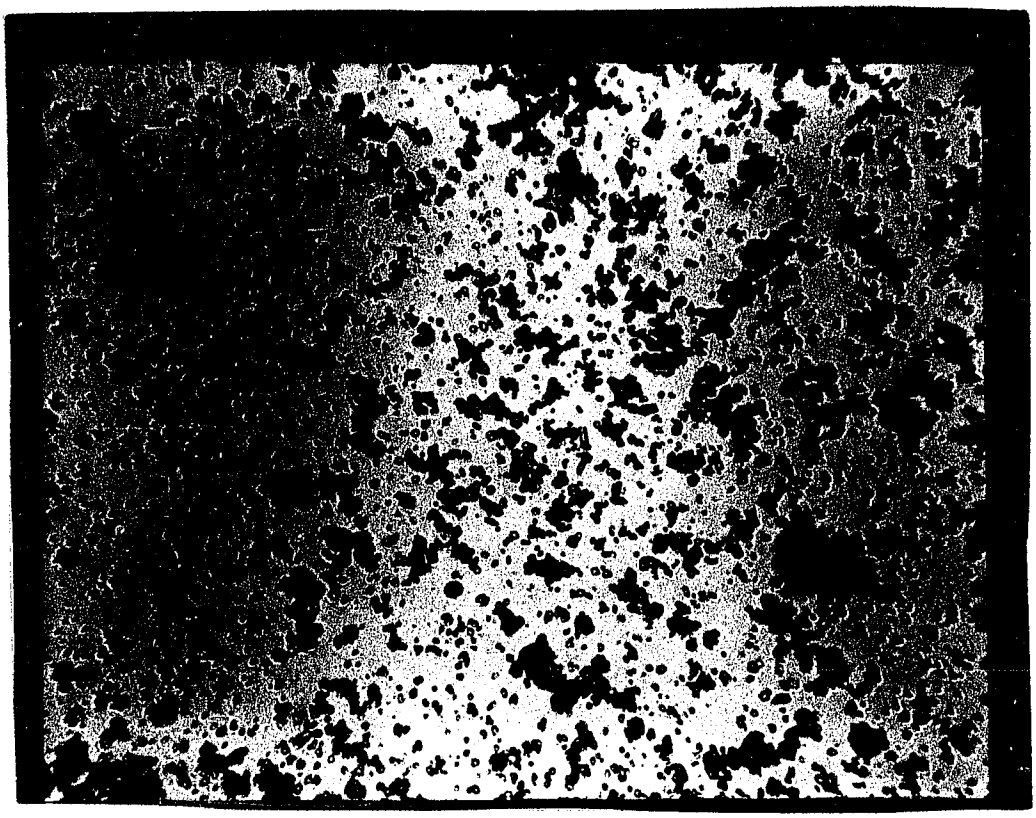

Figure 24. Microphotograph of Crystals from Run 31 (400X)

CHAPTER V

CONCLUSIONS AND RECOMMENDATIONS

On the basis of the experimental results presented in the preceding pages, several conclusions and recommendations may be offered.

1) For the sodium aluminate concentrations studied, a conductometric method for following the decomposition reaction is satisfactory. This method possesses the advantages of being simple and straightforward mechanically, and requiring a minimum of chemical analyses. On the other hand, the conductometric method is limited to essentially isothermal studies. Also, it is difficult to relate a change in conductance directly to a change in aluminate concentration over the entire range of aluminate concentrations.

2) For the concentrations studied, the presence of dissolved sodium oxalate, in industrial oxalate-to-alumina ratios, has little effect on the decomposition of sodium aluminate solutions that are otherwise pure.

3) For the concentrations studied, soluble starch (acting alone) exhibits a significant influence on all phases of the decomposition reaction. High starch concentrations will inhibit decomposition indefinitely. Lower concentrations yield prolonged induction periods, relatively low decomposition rates, high "equilibrium concentrations" of dissolved alumina, and an agglomerated crystal product. These results may be attributed to the shielding or enveloping of potential growth surfaces by the starch.

4) For the concentrations studied, the presence of magnesium, added as $4MgCO_3 \cdot Mg(OH)_2 \cdot 5H_2O$, in otherwise pure sodium aluminate solutions, produces significant effects. This impurity tends to retard the decomposition rates and cause a marked increase in alumina "equilibrium concentrations." Essentially no effects on induction periods and product crystal sizes are noted. These results are interpreted to result from the adsorption of magnesium ions by colloidal aluminum hydroxide particles, with consequent interfering effects on the conversion of this colloidal material to the crystalline product.

5) The validity of extrapolating these results obtained at relatively low concentrations to industrial concentrations (4-6 M NaOH) is unknown. Therefore, it is recommended:

a) that a conductance cell be developed that can adequately follow the reaction at higher concentrations, and

b) that a similar study of the effects of these impurities be made in solutions of higher concentrations.

6) It is possible that the impurities studied (sodium oxalate, starch, magnesium) may interact with one another when simultaneously present in the same sodium aluminate solution to give results that may not be predicted from a knowledge of the effects of the singly acting impurities. Therefore, to advance our understanding of the effects of these impurities on the decomposition of sodium aluminate, it is recommended that studies be made to determine the effects of the various possible combinations of these impurities acting simultaneously.

SELECTED BIBLIOGRAPHY

1. Buckley, H. E., Crystal Growth, John Wiley and Sons, Inc., New York, 1951.

2. Dean, R. B., Modern Colloids, D. Van Nostrand Company, Inc., New York, 1948, pp. 92-132, 162-181, 241-255.

3. Delahay, Paul, Instrumental Analysis, Macmillan Co., New York, 1957, pp. 143-159.

4. Discussions of the Faraday Society, "Crystal Growth," No. 5, 1949.

5. Doremus, R. H., Roberts, B. W., and Turnbull, D., Growth and Perfection of Crystals, John Wiley and Sons, Inc., New York, 1955, pp. 441-5.

6. Evans, R. C., An Introduction to Crystal Chemistry, Cambridge University Press, 1946, pp. 274-301.

7. Frenkel, J., Kinetic Theory of Liquids, Dover Publications, Inc., New York, 1955, Chapter VII.

8. Honeyman, J., Recent Advances in the Chemistry of Cellulose and Starch, Interscience Publishers, Inc., New York, 1959.

9. Ivekovic, H., Vrbaski, T., and Pavlovic, D., "The Precipitation of Alumina Trihydrate from Aluminate Solutions in the Presence of Some Higher Alcohols and Starch," Croat. Chem. Acta 28 (1956), pp. 101-5.

10. Joseph, Olive, "Electrical Conductivities of Solutions Containing Aluminum Hydroxide and Sodium and Potassium Hydroxides," J. Univ. Bombay, Sect. A, 20, Part 3 (Science No. 30), 1951, pp. 39-52.

11. Kerr, R. W., Chemistry and Industry of Starch, Academic Press, Inc. New York, 1944.

12. Kolthoff, I. M. and Sandell, E. B., Textbook of Quantitative Inorganic Analysis, Macmillan Co., 3rd Ed., New York, 1952, pp. 106-137.

13. Kuznetsov, S. I., Antipin, L. N., and Vazhenin, S. F., "Nature of the Variations of Certain Properties of Aluminate Solutions in the Decomposition Process," Journal of Applied Chemistry of U.S.S.R., Vol. 30, No. 3, March, 1957, pp. 377-381 (English translation).

14. Kuznetsov, S. I., Serebrennikova, O. V., and Derevyankin, V. A., "The Influence of Certain Factors on the Decomposition Kinetics of Aluminate Solutions and on the Crystal Size of the Aluminum Hydroxide Obtained,"

Journal of Applied Chemistry of U.S.S.R., Vol. 30, No. 3, March, 1957, pp. 373-376 (English translation).

15. Lewis, W. K., Squires, L., and Broughton, G., Industrial Chemistry of Colloidal and Amorphous Materials, The Macmillan Co., New York, 1942, pp. 175-179.

16. McCabe, W. L., "Crystal Growth in Aqueous Solutions," Industrial and Engineering Chemistry, Vol. 21, 1929, pp. 30, 112.

17. Miers, Sir H. A., "The Growth of Crystals in Supersaturated Solutions," Journal of Institute of Metals, Vol. 37, 1927, pp. 1, 331.

18. Moeller, T., Inorganic Chemistry, John Wiley and Sons, Inc., New York, 1952, pp. 734-757.

19. Newsome, J. W., Heiser, H. W., Russel, A. S., and Stumph, H. C., "Alumina Properties," Technical Paper No. 10, 2nd Revision, Aluminum Company of America, Pittsburgh, Pennsylvania, 1960.

20. "Nucleation Phenomena," Industrial and Engineering Chemistry, Vol. 44, June, 1952, pp. 1269-1338.

21. Pearson, T. G., "The Chemical Background of the Aluminum Industry," Lectures, Monographs and Reports, No. 3, 1955, The Royal Institute of Chemistry, pp. 17-35.

22. Perry, John H., Chemical Engineer Handbook, McGraw-Hill Book Co., New York, 1950, 3rd Ed., pp. 1051-1061.

23. Sato, Taichi, "Studies on the Hydrolysis of Sodium Aluminate Solutions. XVII. Effect of the Addition of Some Carbohydrates on the Particles Precipitated by the Decomposition of Sodium Aluminate Solutions with Seeding," Journal of Applied Chemistry, Vol. 9, 1959, pp. 50-58.

24. Stillwell, C. W., Crystal Chemistry, McGraw-Hill Book Co., Inc., New York, 1938, Chapter 9.

25. Utley, D. W. and Watts, H. L., "Volumetric Analysis of Sodium Aluminate Solutions," Analytical Chemistry, Vol. 25, No. 6, 1953, pp. 864-867.

26. Van Hook, Andrew, Crystallization Theory and Practice, ACS Monograph No. 152, Reinhold Publishing Corp., New York, 1961.

27. Vrbaski, T., Ivekovic, H., and Pavlovic, D., "The Spontaneous Precipitation of Hydrated Alumina from Aluminate Solutions," Canadian Journal of Chemistry, Vol. 36, 1958, p. 1410.

28. Weiser, H. B., Inorganic Colloid Chemistry, Vol. II. The Hydrous Oxides and Hydroxides, John Wiley and Sons, New York, 1935.

29. Wells, A. F., Structural Inorganic Chemistry, 2nd Ed., Clarendon Press, Oxford, 1950, pp. 417-419.

APPENDIX A

NOMENCLATURE AND SYMBOLS

A - Dissolved aluminum concentration, expressed in gpl of equivalent Al_2O_3

Al_2O_3, gpl - Dissolved aluminum concentration, expressed in gpl of equivalent Al_2O_3

C - Caustic soda (NaOH) concentration, expressed in gpl of equivalent Na_2CO_3. All sodium combined as free NaOH and as sodium aluminate is included.

HC - Heavy coarse, referring to a seed charge of 93.5 grams of coarse seed

HF - Heavy fine, referring to a seed charge of 93.5 grams of fine seed

I.D.R. - Initial decomposition rate, expressed as grams of Al_2O_3/hour

LC - Light coarse, referring to a seed charge of 18.7 grams of fine seed

LF - Light fine, referring to a seed charge of 18.7 grams of fine seed

$NaAlO_2$ - Commonly accepted formula for sodium aluminate

Na_2O, gpl - Concentration of all sodium combined as free NaOH and sodium aluminate, expressed as gpl Na_2O

$Na_2O_{tot.}$, gpl - Concentration of all dissolved sodium expressed as gpl Na_2O

Na_2O/Al_2O_3 - The molar ratio of sodium (free NaOH and sodium aluminate), expressed as Na_2O to dissolved aluminum, expressed as Al_2O_3

S.C. - Seed Charge

$\Delta A_{tot.}$ - The difference in A between start and end of a run, gpl Al_2O_3

$\Delta R_{tot.}$ - The difference in resistances at start and end of a run, ohms

$\frac{\Delta R_{initial}}{hr}$ - The slope of the resistance-time curve at the beginning of the decomposition period, ohms/hr

APPENDIX B

DETERMINATION OF CELL CONSTANT[3]

The electrical resistance, R, offered by a given solution to a particular conductance cell may be expressed as

$$R = \frac{1}{k}\frac{\ell}{A} \qquad \text{(B-1)}$$

where R = resistance, ohms

k = specific conductance, ohm^{-1} cm^{-1}

ℓ = interelectrode distance, cm

A = cross sectional area of electrode plate, cm^2

Usually, the cross section (A) and interelectrode distance (ℓ) are not uniform for a particular cell, so the cell constant, ℓ/A, must be determined by measuring R for a solution of known specific conductance. Such standard solutions and their specific conductances are described in several references, one of which is Lange's "Handbook of Chemistry."

For illustrative purposes, a sample cell constant determination is presented below

a) Make up a standard solution of 0.1 N KCl.

b) Immerse cell in this solution.

c) Obtain resistance reading. Assume, for this example, a reading of 27.0 ohms is obtained.

d) Obtain temperature of standard solution. Assume 28°C.

e) From handbook, obtain specific conductance corresponding to this temperature. A .1 N KCl solution at 28.0°C has a specific conductance

of .0137 ohm^{-1} cm^{-1}.

f) Substitute known values into Equation B-1 and solve for cell constant, ℓ/A.

$$27.0 \text{ ohms} = \frac{1}{.01387 \text{ ohm}^{-1} \text{ cm}^{-1}} \left(\frac{\ell}{A}\right)$$

$$\frac{\ell}{A} = .374 \text{ cm}^{-1}$$

APPENDIX C

CALCULATION OF INITIAL DECOMPOSITION RATES

The basis for this calculation is discussed in Section IV-1. A sample calculation (for Run 5) is presented below.

$V = 4$ liters

$\Delta A_{tot.} = 30.6 - 17.0 = 13.6$ gpl

$\Delta R_{tot.} = 2.83 - 2.25 = .58$ ohms

$$\frac{\Delta R_{initial}}{hr} \quad \frac{2.83 - 2.31}{8.0 - .75} = \frac{.52}{7.25} = .0718 \text{ ohms/hr}$$

$$\text{I.D.R.} = \left(\frac{\Delta R_{initial}}{hr}\right)\left(\frac{\Delta A_{tot.}}{\Delta R_{tot.}}\right)(V)$$

$$= (.0718)\left(\frac{13.6}{.58}\right)(4) \text{ gm } Al_2O_3/hr$$

$$= 6.7 \text{ gm } Al_2O_3/hr$$

APPENDIX D

SEED SPECIFICATIONS

All trihydrate seed was obtained from Kaiser Aluminum's Baton Rouge Works. The following information was provided by Kaiser:

Chemical Analyses

	Fine Seed	Coarse Seed
Loss on Ignition	34.76%	34.73%
Insolubles	.03	.05
CaO	.03	-
SiO_2	.004	.004
Fe_2O_3	.003	.007
Na_2O_3	.28	.21

Screen Sizes

Screen	Fine Seed	Coarse Seed
+100	0 %	33.2%
-100 to +140	1.4	37.6
-140 to +200	5.6	14.8
-200 to +325	16.0	13.4
-325	77.0	1.0
S_w, cm^2/gm	1300	391.5
D_m, mean diameter, microns	21	69

APPENDIX E

CHEMICAL TERMINOLOGY[18,19,28]

The following terminology is frequently encountered in literature pertinent to the production of alumina:

1. γ-$Al_2O_3 \cdot 3H_2O$ (gibbsite, hydrargillite) -- The stable 3-hydrate. This form is found as a mineral and is obtained by rapid hydrolysis of an aluminate solution. It has a monoclinic crystal system and a specific gravity of 2.42.

2. α-$Al_2O_3 \cdot 3H_2O$ (bayerite) -- Metastable with respect to gibbsite but stable with respect to boehmite. Obtained by aging boehmite gel under dilute alkali or by slow hydrolysis of an aluminate solution.

3. α-$Al_2O_3 \cdot H_2O$ (diaspore) -- A naturally occurring material with an orthorhombic crystal system and a specific gravity of 3.44.

4. γ-$Al_2O_3 \cdot H_2O$ (boehmite) -- A material stable in steam at 400°C. It is precipitated from boiling aluminum salt solutions by ammonia. Also obtained as the first product of the aging of amorphous gel thrown down by alkalies at room temperatures, or by aging gibbsite at 350°C in a hydrothermal bomb. Boehmite has an orthorhombic crystal system and a specific gravity of 3.01.

5. Hydrated oxide -- Contains stoichiometrically proportioned combined water.

6. Hydrous oxide -- An oxide containing varying amounts of water, e.g., what is commonly referred to as $Fe(OH)_3$ is actually a hydrous oxide, $Fe_2O_3 \cdot \pm 20H_2O$.

7. Hydrous hydrated oxide -- A hydrated oxide which adsorbs varying amounts of water.

8. Hydrous hydroxide -- Contains elements of water combined in the form of a hydroxide, such as $Be(OH)_2$, $CO(OH)_2$ and $Fe(OH)_2$.

APPENDIX F

DESCRIPTION OF SIEVES

The following sieves were used to obtain size distributions of the product crystals from the various runs:

NBS No.	Opening, microns	Opening, inches
35	500	.0197
100	149	.0059
140	105	.0041
200	74	.0029
230	62	.0024

APPENDIX G

RESISTANCE-VS-TIME DATA

Run	Time, hr	Temp., °C	Resistance, ohms
5	0 (S.C.)		2.83
	.25		2.83
	.5		2.83
	.75	70.0	2.83
	1		2.81
	1.25		2.78
	1.5		2.75
	2		2.74
	2.5	70.1	2.72
	3		2.68
	3.75		2.63
	4.5		2.59
	5.25		2.55
	6		2.51
	7		2.48
	8	70.0	2.45
	10		2.41
	11		2.38
	13		2.35
	14		2.34
	23.75		2.25
	27.75		2.25
	29	70.0	2.25
6	0 (S.C.)		2.83
	.25		2.82
	.5	69.9	2.75
	.75		2.73
	1		2.71
	1.25		2.69
	1.5		2.66
	1.75		2.63
	2	70.0	2.61
	2.5		2.56
	3		2.53
	3.5		2.51
	4		2.49
	4.5	70.0	2.47
	5		2.45
	6.5		2.41

APPENDIX G (Continued)

Run	Time, hr	Temp., °C	Resistance, ohms
6 (Contd.)	7.75		2.38
	8.75		2.36
	10.5		2.32
	11.75		2.31
	19.25	70.0	2.23
	20.5		2.22
	22		2.21
	24		2.21
	26		2.21
	28	70.0	2.21
7	0 (S.C.)		2.83
	.25		2.79
	.5	69.9	2.74
	.75		2.71
	1		2.69
	1.25		2.64
	1.5		2.62
	1.75		2.61
	2		2.58
	2.25		2.55
	2.5		2.53
	3	70.0	2.50
	4.25		2.46
	5		2.43
	6		2.41
	7		2.39
	8		2.36
	17		2.26
	18		2.25
	20		2.24
	21.75	70.0	2.22
	24		2.22
	26		2.22
8	0		2.85
	.25		2.68
	.5	70.0	2.57
	.75		2.51
	1		2.46
	1.25		2.43
	1.5		2.41
	2		2.36
	2.5		2.34
	3.25	70.0	2.28
	4.75		2.25
	6.25		2.22
	8		2.21

APPENDIX G (Continued)

Run	Time, hr	Temp., °C	Resistance, ohms
8 (Contd.)	9		2.20
	18		2.16
	19.5		2.16
	21		2.16
	26.5	70.1	2.16
9	-1 (ox.chg.)		2.78
	0 (S.C.)		2.78
	.25		2.78
	.5	70.0	2.78
	.75		2.78
	1		2.78
	1.25		2.78
	1.5		2.76
	1.75		2.74
	2		2.73
	2.25		2.74
	2.5		2.70
	2.75		2.68
	3		2.67
	3.25		2.65
	3.5		2.64
	4		2.60
	4.5		2.57
	5	70.0	2.56
	7		2.46
	9		2.40
	18.25		2.27
	20		2.26
	22		2.26
	24.25		2.24
	26.5		2.24
	27.75		2.24
	30.75	70.0	2.22
10	-2 (ox.chg.)	69.7	2.78
	0 (S.C.)	70.0	2.78
	.25		2.77
	.5		2.74
	.75		2.69
	1		2.67
	1.25	70.0	2.65
	1.5		2.63
	2		2.58
	2.5		2.55
	3		2.51
	3.5		2.48
	4.25	70.0	2.46

APPENDIX G (Continued)

Run	Time, hr	Temp., °C	Resistance, ohms
10 (Contd.)	6.5		2.38
	7		2.37
	9	70.0	2.33
	18.75		2.24
	21		2.23
	22.75		2.23
	25.25		2.22
11	-.25 (ox.chg.)		2.79
	0 (S.C.)		2.79
	.25	69.9	2.79
	.5		2.77
	.75		2.74
	1		2.71
	1.25		2.67
	1.75		2.63
	2		2.59
	2.5	70.0	2.55
	3		2.52
	3.5		2.48
	4.25		2.46
	6.25		2.37
	8.5		2.34
	10		2.29
	10.75		2.28
	19.25		2.24
	21		2.23
	23		2.22
	27.5	70.0	2.22
12	-1 (ox.chg.)		2.78
	0 (S.C.)		2.78
	.25		2.67
	.5		2.58
	.75	70.1	2.53
	1.5		2.44
	2		2.37
	2.25		2.35
	3		2.32
	3.75		2.29
	6.5		2.24
	8		2.22
	9		2.21
	19	70.0	2.18
	22.75		2.17
	28		2.17

APPENDIX G (Continued)

Run	Time, hr	Temp., °C	Resistance, ohms
13	0 (s.c.)		2.86
	.25		2.86
	.5		2.86
	.75	70.0	2.85
	1		2.83
	1.25		2.80
	1.75		2.77
	2		2.75
	2.25		2.74
	4		2.63
	4.5		2.60
	5		2.56
	6.5		2.51
	8.5		2.44
	9.75		2.40
	21.25	70.0	2.27
	23		2.26
	26.5		2.25
14	0 (s.c.)		2.86
	.25	70.0	2.81
	.5		2.77
	.75		2.74
	1		2.69
	1.25		2.67
	1.5		2.66
	1.75		2.64
	2		2.61
	3.25		2.54
	5.25		2.46
	7		2.39
	7.5		2.38
	18.75		2.27
	21		2.25
	23	70.0	2.25
	26.5		2.25
15	0 (s.c.)		2.86
	.25		2.85
	.5	69.9	2.78
	.75		2.76
	1		2.73
	1.25		2.68
	1.5		2.66
	1.75		2.64
	2		2.60
	2.5		2.57
	3	70.0	2.54

APPENDIX G (Continued)

Run	Time, hr	Temp., °C	Resistance, ohms
15 (Contd.)	4		2.48
	7		2.38
	8	70.0	2.36
	20.25		2.24
	26.5		2.23
16	0 (S.C.)		2.86
	.25		2.72
	.5		2.63
	.75		2.56
	1	70.1	2.51
	1.25		2.47
	3.5		2.34
	6		2.26
	17.5		2.21
	20		2.20
	26.5	70.0	2.20
17	-.5 (starch chg.)	69.9	2.91
	0 (S.C.)		2.91
	.25	70.0	2.91
	20.5	70.0	2.91
18	-.5 (starch chg.)		2.85
	0 (S.C.)	70.0	2.85
	10.25		2.85
19	-.5 (starch chg.)		2.93
	0 (S.C.)	70.0	2.93
	.25		2.85
	.5		2.77
	.75		2.73
	1		2.68
	1.25		2.65
	1.5		2.63
	2.25		2.56
	3		2.52
	3.5		2.49
	5		2.45
	6		2.43
	7		2.41
	9		2.37
	12	70.0	2.35
	24		2.30
	25.5		2.30
	26.5		2.30

APPENDIX G (Continued)

Run	Time, hr	Temp., °C	Resistance, ohms
20	-.5 (starch chg.)		2.85
	0 (S.C.)		2.85
	.25		2.85
	.5		2.85
	.75	70.0	2.85
	1		2.85
	1.25		2.85
	1.5		2.85
	1.75		2.85
	2		2.85
	2.25		2.85
	3		2.85
	3.25		2.85
	3.75	70.0	2.85
	4.25		2.85
	4.75		2.85
	5.75		2.82
	6		2.78
	6.25		2.77
	6.75		2.75
	8.5		2.72
	11.25		2.60
	11.75		2.57
	12.25		2.55
	22		2.40
	23		2.38
	24	70.0	2.37
	26		2.36
	28		2.36
21	-.25 (Mg chg.)		2.85
	0 (S.C.)		2.85
	.25	69.9	2.75
	.5		2.65
	.75	70.0	2.61
	1		2.57
	1.5		2.52
	2		2.47
	2.5		2.45
	3		2.44
	4.5		2.38
	5.5		2.37
	7	70.0	2.36
	8.5		2.36
	11.75		2.36
	24		2.36
	27		2.36

APPENDIX G (Continued)

Run	Time, hr	Temp., °C	Resistance, ohms
22	-.25 (Mg chg.)		2.85
	0 (S.C.)	70.0	2.85
	.25		2.85
	.5		2.83
	.75		2.77
	1		2.75
	1.25		2.74
	1.5		2.73
	2		2.67
	2.75		2.64
	3.5		2.61
	4	70.0	2.57
	5.5		2.52
	6.5		2.50
	7.25		2.48
	9.25		2.45
	11.5		2.44
	13.5		2.42
	25.5		2.39
	26.5		2.39
23	-.25 (Mg chg.)		2.85
	0 (S.C.)		2.85
	.25		2.85
	.5		2.83
	.75		2.78
	1		2.76
	1.5		2.74
	2		2.71
	2.5	70.0	2.67
	3		2.65
	4.25		2.57
	5.25		2.55
	6		2.54
	7		2.54
	8.25		2.53
	10.25		2.52
	11.75		2.51
	23.5		2.50
	26.5		2.50
24	-.25 (Mg chg.)		2.83
	0 (S.C.)		2.83
	.25		2.83
	.5	70.0	2.83
	.75		2.83
	1		2.81
	1.5		2.79

APPENDIX G (Continued)

Run	Time, hr	Temp., °C	Resistance, ohms
24 (Contd.)	2	69.9	2.76
	2.5		2.75
	3		2.74
	4.25		2.71
	5	70.0	2.68
	6		2.65
	7		2.63
	8.5		2.58
	10.5		2.53
	12.25		2.46
	23.5		2.46
	25		2.46
	26.5		2.46
25	-.25 (Mg chg.)	70.0	2.85
	0 (S.C.)		2.85
	.25		2.83
	.5		2.77
	.75		2.75
	1		2.73
	1.5		2.68
	2		2.65
	2.5		2.61
	3		2.57
	3.5		2.55
	4.5		2.52
	5.5		2.48
	6.25		2.45
	7.25	70.0	2.44
	9.75		2.43
	12.25		2.41
	24		2.38
	26.5		2.38
26	-.25 (Mg chg.)		2.85
	0 (S.C.)		2.85
	.25		2.84
	.5		2.79
	.75		2.75
	1		2.73
	1.5		2.67
	2	70.0	2.64
	3		2.57
	4		2.54
	5		2.48
	6		2.46
	7		2.45
	8		2.44

APPENDIX G (Continued)

Run	Time, hr	Temp., °C	Resistance, ohms
26 (Contd.)	10.25		2.39
	12.75		2.37
	23.5		2.35
	26.75		2.35
27	-.25 (Mg chg.)		2.85
	0 (S.C.)		2.85
	.25		2.84
	.5		2.77
	.75		2.75
	1		2.73
	1.5		2.68
	2.25	70.0	2.63
	3.5		2.55
	4.5		2.51
	5.25		2.48
	6.5		2.45
	8		2.42
	11		2.36
	12		2.35
	24.25		2.27
	26.75		2.27
28	-.5 (starch chg.)		2.85
	0 (S.C.)		2.85
	.25		2.85
	.5		2.85
	.75		2.85
	1	70.0	2.82
	1.25		2.78
	1.5		2.76
	2		2.73
	2.5		2.71
	3.5		2.65
	4.5		2.61
	5.5		2.56
	6.5		2.53
	8		2.49
	10.5		2.45
	13		2.40
	24.5		2.28
	26.5		2.27
29	-.5 (starch chg.)		2.89
	0 (S.C.)		2.85
	.25		2.85
	.5		2.85
	.75		2.85

APPENDIX G (Continued)

Run	Time, hr	Temp., °C	Resistance, ohms
29 (Contd.)	1		2.85
	1.25		2.85
	1.5	70.0	2.85
	1.75		2.85
	2		2.85
	2.25		2.85
	2.5		2.82
	2.75	70.0	2.79
	3		2.77
	3.25		2.75
	4.5		2.71
	5.5		2.67
	6.5		2.64
	7.5		2.62
	10		2.57
	12		2.54
	23.5		2.40
	26		2.39
	30.5		2.38
30	-.5 (starch chg.)		2.85
	0 (S.C.)		2.85
	.25		2.85
	.5		2.83
	.75		2.79
	1		2.76
	1.5		2.73
	2	70.0	2.68
	2.5		2.65
	4.5		2.55
	6		2.48
	8.25		2.44
	10		2.37
	12		2.35
	25		2.27
	27		2.25
31	0		5.77
	24	30.8	5.77
	48		5.77
	65		5.77
	72	30.8	5.75
	96		5.65
	168		5.10
	192		4.55
	209	30.7	4.40
	233		4.28
	257		4.22

AUTOBIOGRAPHY

The author was born December 20, 1932, in New Orleans, Louisiana. He received his elementary education in that city and graduated from high school at New Orleans Academy in 1950. In 1954 he received the degree of B.S. in Chemical Engineering from Tulane University. The next two years were spent in military service as an instructor at The Engineer School, Fort Belvoir, Virginia. After being released from active duty in 1956, he acquired two years of chemical engineering experience in the alumina industry with Kaiser Aluminum and Chemical Corporation and Ormet Corporation. In February, 1959, the author entered the Graduate School of Louisiana State University, where he received the degree of M.S. in Chemical Engineering in 1960. At present, he is a candidate for the degree of Doctor of Philosophy in Chemical Engineering at that same institution.

EXAMINATION AND THESIS REPORT

Candidate: James Leslie Kelly

Major Field: Chemical Engineering

Title of Thesis: A STUDY OF THE INFLUENCES OF BAYER PROCESS IMPURITIES ON THE CRYSTALLIZATION OF ALUMINA TRIHYDRATE

Approved:

Major Professor and Chairman

Dean of the Graduate School

EXAMINING COMMITTEE:

Date of Examination:

May 18, 1962